Early View publication on www.wileyonlinelibrary.com
(issue and page numbers not yet assigned;
citable using Digital Object Identifier – DOI)

LASER & PHOTONICS REVIEWS

Laser Photonics Rev., 1–21 (2010) / **DOI** 10.1002/lpor.201000012

Abstract Metamaterial research is an extremely important global activity that promises to change our lives in many different ways. These include making objects invisible and the dramatic impact of metamaterials upon the energy and medical sectors of society. Behind all of the applications, however, lies the business of creating metamaterials that are not going to be crippled by the kind of loss that is naturally heralded by use of resonant responses in their construction. This review sets out some solutions to the management of loss and gain, coupled to controlled and nonlinear behavior, and discusses some critical consequences concerning stability. Under the general heading of active and tunable metamaterials, an international spectrum of authors collaborates here to present a set of solutions that addresses these issues in several directions. As will be appreciated, the range of possible solutions is really fascinating, and it is hoped that these discussions will act as a further stimulus to the field.

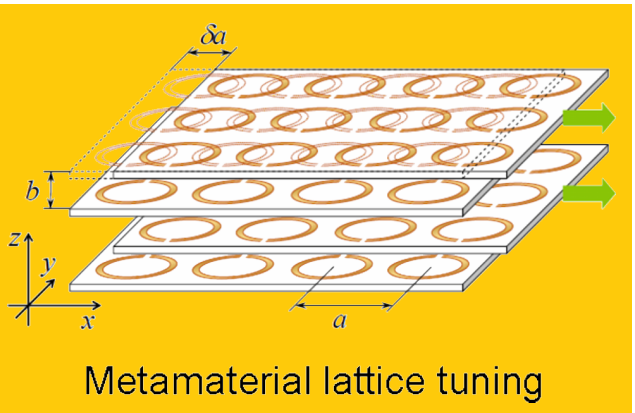

Active and tunable metamaterials

Allan D. Boardman[1,*], Volodymyr V. Grimalsky[2], Yuri S. Kivshar[3], Svetlana V. Koshevaya[2], Mikhail Lapine[4], Natalia M. Litchinitser[5], Vadim N. Malnev[6], Mikhail Noginov[7], Yuriy G. Rapoport[1,8], and Vladimir M. Shalaev[9]

1. Introduction

As pointed out in 1970, in the seminal book by Scott [1] on active and nonlinear wave propagation in electronics, there was, by that time, research stretching back to the 1950s on devices such as traveling-wave tubes and backward-wave oscillators [2]. The latter, involving electrons travelling in the opposite direction to the electromagnetic energy. This means that the appearance of backward waves in isotropic metamaterials is not so surprising. Nevertheless, the latter, because of this property, can sustain, the kind of negative refraction, which surprised everybody and generated a massive global excitement in the last decade [3, 4]. All of the early electronic devices involved *active* and, possibly, nonlinear processes [1], with the word *active* meaning that some extrinsic, or intrinsic, *action* is being added to an original passive design. The actions can include an intrinsic energy source that creates amplification to combat loss, or an interrogation of the device with an external source of energy, such as a laser beam [1]. In addition, many forms of control can be accessed by putting the device under an externally applied influence, such as a constant magnetic field [5], or by incorporating into the device a feature that permits significant control over its resonant behavior [6, 7].

Metamaterials derive their behavior from combinations of effective permittivity and effective permeability that arise as a consequence of averaging over the behavior of a set of metaparticles. These metaparticles could be nanoparticles, or wires and resonators, and the latter can possess a wide variety of formats, ranging from split-ring assemblies to being shaped like an S, or even the Greek letter omega [8]. They can also be nanowire pairs [9]. If no *action* is taken, or nothing else is added to these kinds of metaparticle then the resultant metamaterial remains in a *passive* state. A major consequence of this would be to suffer significant loss in the resonance-frequency window, which is precisely where many device operations are optimized. This situation could be ameliorated by moving the loss and gain windows relative to each other [10]. The more general point, however, is that it is necessary to adopt an *active* design that involves an *intervention* to the passive design that will enable a lot of practical applications to appear on the horizon of possi-

[1] Joule Physics Laboratory, Institute for Materials Research, University of Salford, Salford, Greater Manchester, United Kingdom [2] Autonomous University of Morelos, Av. Universidad, 1001, Z. P. 62210, Cuernavaca, Morelos, Mexico [3] Nonlinear Physics Center, Research School of Physics and Engineering, Australian National University, Canberra ACT 0200, Australia [4] Department of Electronics and Electromagnetics, University of Seville, Spain [5] Department of Electrical Engineering, The State University of New York at Buffalo, Buffalo, New York 14260, USA [6] Department of Physics, Addis Ababa University, Addis Ababa 1176, Ethiopia [7] Center for Material Research, Norfolk State University, Norfolk, Virginia 23504, USA [8] Physics Faculty, Taras Shevchenko Kyiv National University, Prospect Glushkov 6, 22 Kyiv, Ukraine [9] School of Electrical and Computer Engineering and Birck Nanotechnology Center, Purdue University, West Lafayette, Indiana 47907, USA
[*] Corresponding author: e-mail: a.d.boardman@salford.ac.uk

bilities. These include, "perfect lenses" [3], delay lines [11], filters, antennae substrates [12], nonlinear guided wave applications [13, 14] and circuit models [15]. The fact that overcoming loss is a most important contemporary question is now well understood but the solution of this problem will also lead to the brilliant possibility that a metamaterial will also be able to amplify electromagnetic waves [16–18].

The present article brings together some views on "active metamaterials" in which either some sources of energy may be introduced solely for wave gain [17, 19] and loss compensation, or the possibility of active control is elucidated. Such control could be exercised by embedding into a metaparticle, a tunable electronic component [6, 7].

Referring back to the extensive literature on plasma physics, geophysics, astrophysics, solid-state physics, and microwave engineering, reveals that active media have been rigorously investigated in the past [20–22]. In recent times, for metamaterials, it has been suggested that gain can be added to a system by means of parametric optical amplification [19], loading metaparticles with active devices such as diodes [18, 23], doping metamaterials with quantum dots [24], or adding dyes for amplification of plasmonic behavior [25]. Approaches to amplification of electromagnetic waves in metamaterials and their stability consequences will be introduced below in some detail.

In this context, the classical nonlinear optical parametric amplification [26] approach can be elegantly modified to embrace negative phase metamaterials (a name given to so-called double-negative metamaterials, for which *both* the relative permittivity and relative permeability are negative). In particular, if an electromagnetic wave can access a second-order nonlinearity of a metamaterial, then it is possible to satisfy the corresponding specific synchronism conditions [27] in a novel way. Indeed, a three-wave parametric coupling takes place that can be organized to produce amplification in the visible optical range.

The latter range also embraces plasmonic metamaterials [28–31] that are being widely investigated now, such as those based on pairs of coupled nanowires, periodic arrays consisting of stacked metallic nanorods, arrays of metal nanopillar pairs, and two-dimensional arrays of metallic cylinders [32]. Plasmon resonance is a very important factor in the functioning of metamaterial nanocomposites [33]. Indeed, surface plasmon–polariton properties can provide typical metamaterial functionality in subwavelength focusing [32] and can be applied to the creation of circuit elements at optical frequencies [34], or used for integrated optical metamaterial waveguides and for many other metamaterial applications. Because of this relevance, amplification of surface plasmon polaritons using embedded dyes, in particular, is also presented in this review.

It is of fundamental practical importance to determine whether waves in the bulk, in waveguide structures, and metaparticle arrays in active systems are stable, or unstable, in either linear and nonlinear systems. This may seem an obvious question to pose but it is seldom addressed and yet once a system becomes active it is necessary to do so. If the system is linear, the principle of superposition is valid and any instability (either absolute, or convective [35–37]) can be investigated using a form of Fourier analysis. Then, simply speaking, the question is, whether amplification, or generation, can take place in an active system, so that spatial amplification is a possible outcome, for example. If so, it is necessary to *avoid* absolute instability, and wave generation. Also, a perturbation growing in the system, in the linear stage of instability, with maximum increment (time rate), can become a seeding factor for further development of nonlinear perturbations [38, 39]. Moreover, linear decay of interesting entities like solitons can be partially overcome, or their amplitude can be even increased, in definite frequency ranges due to linear gain in an active nonlinear system. Therefore, linear instability is related strongly to the nonlinearity that the system may sustain. This is an important point if the observation time, or system length, is large enough to allow nonlinearity to develop. Concerning the linear regime, the concept of absolute and convective instabilities and spatial gain [35–37], will be considered here for metamaterials, based on metaparticles with embedded active components (diodes). For the nonlinear regimes, attention will be restricted here to a demonstration of the possibility of gain (spatial amplification). More general methods, involving a search for stability in active nonlinear systems [1, 40, 41] will be discussed in later publications.

In addition to the work described above, the principle of amplification, connected to superheterodyne amplification in a layered metamaterial–semiconductor–metamaterial structure, will also be introduced. The basis of this method is an effective transfer of amplification from low-frequency (space charge) waves [42, 43], in a semiconductor with a negative differential conductivity, to a high-frequency infrared wave. The essential point is that the process exploits any intrinsic negative-phase behavior of a material. Even though the corresponding wave interactions are nonlinear, and high-frequency pumping is necessary, the nonlinearities are confined entirely to the semiconductor, and therefore the metamaterials constituents can be linear. This method can be used over broad frequency ranges and needs only moderate, or even, relatively, low pumping power. Following this topic, the article continues with the possibility of controlling the characteristics of metamaterials with active/nonlinear electronic devices [6, 23, 44] embedded in the metaparticles.

The discussion will now continue with a more detailed investigation of how the familiar nonlinear optics topic, called optical parametric amplification (OPA) can be exploited to enhance metamaterial viability.

2. Loss control through sources of gain or optical parametric amplification

The desire to create metamaterial applications that are free of debilitating loss has been outlined in the introduction and the optical frequency window is especially attractive for applications, has led to the development of photonic metamaterials that often take a route based upon metal–dielectric engineered structures [45], and losses in such structures must be expected and must be expected to have various origins, some of which are still not completely quantified.

Some known sources of loss in photonic metamaterials, however, stem from surface roughness, quantum size and chemical interface effects, the resonant nature of their magnetic response, or relate to the fundamental loss properties of their constitutive components—metals [46]. Therefore, various approaches to the realization of low-loss metamaterials have been taken, including advancements in fabrication techniques [47], development of novel metamaterials designs [48], and the incorporation of gain material in the metamaterials structures [49]. The use of optical amplification [19, 27, 49] is a fascinating possibility, however, so the principles underpinning this will now be elucidated. Although the emphasis here is upon metamaterials, it is encouraging to learn that loss reduction using optical amplification has a long history in photonics, especially in the context of optical telecommunications. The latter uses rare-earth-doped gain media, semiconductor materials, or accesses nonlinear effects such as stimulated Raman and Brillouin scattering, four-wave mixing and optical parametric amplification [50].

In the context of metamaterials, before a nonlinear optical parametric amplification approach is developed here, it should be pointed out that among the first conceptual approaches to managing losses in metamaterials is the use of a stack of alternating negative and positive index layers [51, 52]. The use of such a stack considerably reduces the loss experienced by an electromagnetic wave, compared to what it would encounter in a bulk negative-phase medium (NIM). Naturally, improved outcomes soon emerged. For example, using positive index gain materials as layers by deploying optically pumped semiconductors [53]. A very recent achievement [54] uses a fishnet structure that incorporates gain material into high local field areas and the outcome is *extremely* low loss.

Before the fishnet work a paradigm early example of manipulating gain [55] deployed double silver strips actually embedded into a gain medium, as sketched in Fig. 1a. After exposing this structure to a plane wave with a wavelength of 584 nm, the transmission and reflection results shown in Fig. 1b clearly emerge as functions of gain.

In this kind of work, the gain is linearly sourced from dye molecules (e. g., Rhodamine 6G) or semiconductor quantum dots (e. g., CdSe) applied to the top of the negative-phase medium (NIM). Alternatively, replacing the dielectric Al_2O_3 with gain material significantly reduces the required gain because of the enhanced local fields in that area.

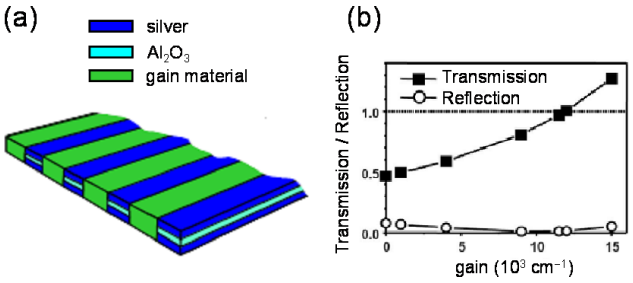

Figure 1 (online color at: www.lpr-journal.org) (a) Negative-index structure made from double silver strips immersed into a gain medium, (b) The transmission and reflection outcomes as functions of gain. Adapted from [55].

The approaches just highlighted can be replaced by optical parametric amplification (OPA) that is enabled by special "backward" phase-matching conditions [19, 27, 49]. "Backward" phase matching results from one of the most fundamental properties of NIMs, namely antiparallel wave and Poynting vectors, i. e. phase and group velocities.

An examination of the effective permittivity and effective permeability of an isotropic metamaterial shows that it may possess NIM properties in some frequency range and positive-index material (PIM) properties at other frequencies. This leads to the basic idea of loss compensation by exploiting electromagnetic waves with the frequencies *outside* the negative-index frequency range to provide loss-balancing OPA at frequencies *inside* the negative index of refraction range. One possibility is to rely upon second-order ($\chi^{(2)}$) nonlinearity of the NIM [19, 27]. Another possibility can be based upon a four-wave interaction process in a medium that displays $\chi^{(3)}$ (cubic)-nonlinearity, e. g., embedded four-level centers, that can be controlled independently from the NIM parameters. This enables the realization of frequency-tunable transparency windows in NIMs [49].

In the example shown here, a strong pump field is allowed to propagate in the positive-index frequency window at a frequency ω_3, while a weak signal is allowed to propagate in the negative-index regime at a frequency ω_1. This action generates an idler wave with a frequency $\omega_2 = \omega_3 - \omega_1$ that is also located in the positive-index region. The idler feeds back to the input signal through the three-wave mixing process, $\omega_1 = \omega_3 - \omega_2$, and produces optical parametric amplification through a coherent energy transfer from the pump field to the signal. This is backward phase-matched as shown in Fig. 2a. Fig. 2b shows extraordinary resonant behavior of the signal transmission as a function of intensity of the pump field g and the NIM slab thickness L, indicating that the amplification can entirely compensate for the absorption and, remarkably, and even turn into oscillations without the need for a cavity. These oscillations result from the effective distributed feedback enabled by the backward-wave nature of the system that essentially has phase and group velocities, oppositely directed. Hence, each spatial point serves as a source for a generated wave travelling in the reflected direction, whereas the phase velocities of all the interacting waves are actually moving in the same direction.

It is interesting that the resonances shown in Fig. 2b are rather narrow. This implies the sample remains opaque if any deviation from the specific parameters (pump intensities and slab thicknesses) occurs that is associated with those resonances. However, a remarkable regime of the OPA in NIMs has been discovered [56] suggesting that the transmission of an NIM slab at a signal frequency ω_1 can be transformed, increased to nearly 100% and even turned into amplification within a broad range of intensities of the pump fields and the slab thicknesses. This is achieved by adjusting the level of absorption at the idler frequency ω_2, as shown in Fig. 2c. Surprisingly, the *absorption coefficient* α_2 at the idler fre-

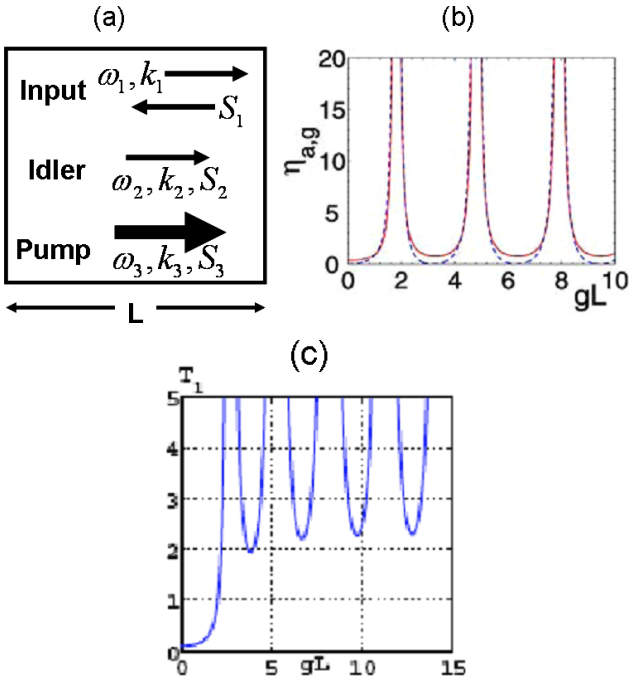

Figure 2 (online color at: www.lpr-journal.org) (a) A schematic of the optical parametric amplification (OPA) for a slab of negative-index material (NIM) of thickness L, ω_1: input signal, ω_2: idler, ω_3: pump. (b) Signal transmission for $\alpha_1 L = 1$, $\alpha_2 L = 0.5$, where η_a is the amplification factor (solid line) and η_g is the conversion factor for the idler wave (dashed line). (c) Signal transmission $\alpha_1 L = 2.3$, $\alpha_2 L = 4$. Adapted from [27, 55].

quency ω_2 has to be *increased* so that $\alpha_2 \geqslant \alpha_1$, where α_1 *is the absorption coefficient* at the signal frequency ω_1.

Promising approaches, such as those discussed above, continue to be pursued and within the broad field of discussions about gain, it is recognized that plasmonic properties of metamaterials need to be thoroughly addressed. This quest is the underpinning basis of the next section.

3. Gain of surface plasmon polariton waves

The construction of metaparticles using wires and split rings, for example, means that the properties of many metamaterials critically depend upon *surface plasmons,* especially as the optical frequency window is approached. The latter are oscillations of free electrons localized at a metallic surface, and have a plasma frequency associated with the size and, mainly, the shape of the particle [57–59]. Electromagnetic surface modes with a photon–plasmon content are called surface plasmon–polaritons. Such a surface electromagnetic wave can propagate along the interface between two media possessing permittivities with opposite signs, such as metals and dielectrics [60, 61]. An investigation of those kinds of waves is relevant because such resonant plasma oscillations determine the properties of many metamaterials and metamaterial-based devices.

Most of the existing and potential future applications of nanoplasmonics suffer from damping caused by metal absorption, however. Hence, once again, significant compensation of surface plasmon–polariton loss through the introduction of gain and the creation of stimulated emission of surface plasmon–polaritons (SPP) needs to be addressed. Before this is done it is fascinating to note that [62] a localized surface plasmon resonance in a metallic nanosphere can exhibit a singularity, when the interfacing dielectric has a critical value of optical gain. Indeed, this phenomenon is relevant to the theoretically proposed SPASER that generates stimulated emission of surface plasmons to resonating a metallic nanostructure adjacent to a gain medium [63].

It is possible to compensate loss in metal with gain by using a mixture of silver nanoparticles and rhodamine 6G dye. The quality factor of surface plasmon resonance increases, as witnessed by a six-fold enhancement of Rayleigh scattering [25, 64]. In the next few sections, because of the importance of being able to control plasmonic phenomena associated with metamaterials, the central discussions will be about how to devise means of controlling losses. It is well known [61] that surface modes can be readily produced in the laboratory by attenuating the total reflection within a prism arrangement. This is called the method of attenuated total reflection (ATR) and will be discussed later. First, however, some details of how to conquer surface plasmon loss will be given.

3.1. Conquering surface plasmon loss in a Ag aggregate by optical gain sourced from a dielectric medium

A fractal aggregate of silver nanoparticles can be treated, in the first approximation, as a collection of spheroids, with different aspect ratios, formed by nanoparticle chains of different lengths [65]. Also, the gain $\sim 10^3$ cm^{-1} needed to compensate the surface plasmon loss is within the limits of semiconducting polymers [66], highly concentrated laser dyes [62], or quantum dots.

A study of Rayleigh scattering in the mixtures of R6G dye (Rhodamine 590 Chloride) and fractal aggregates of Ag nanoparticles [25] has been used. The absorption spectrum of the Ag aggregate has one structureless band covering the whole visible range and extending to the near-infrared. The major feature in the absorption (emission) spectrum of R6G is a band peaking at ≈ 528 nm.

In the reported pump-probe Rayleigh scattering experiments, R6G-Ag aggregate mixtures have been pumped with a frequency-doubled Q-switched Nd:YAG laser ($\lambda_{\text{pump}} = 532$ nm, $t_{\text{pump}} \approx 10$ ns).

In order to achieve the results in Fig. 3, a fraction of the pumping beam was split off and used to pump a simple laser consisting of the cuvette with R6G dye placed between two mirrors, Fig. 3 (upper inset). Its emission wavelength (~ 558 nm) corresponded to the maximum of the gain of R6G dye in the mixtures studied. The beam of the R6G laser, which was used as a probe in the Rayleigh scattering experiment, was collinearly aligned with the pumping beam and sent to the sample through a small (0.5 mm) pinhole.

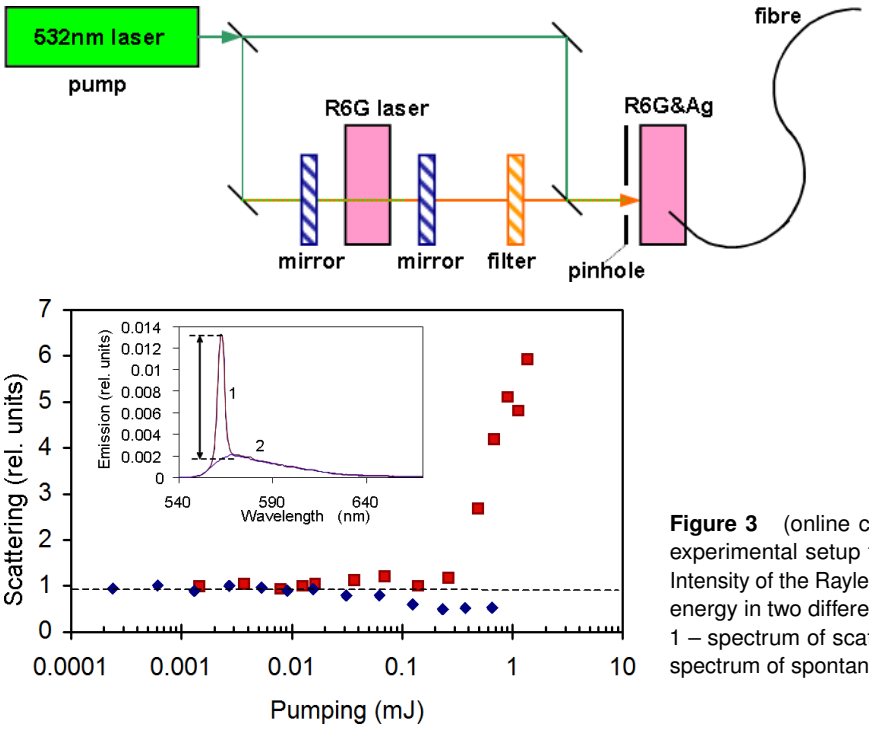

Figure 3 (online color at: www.lpr-journal.org) Pump-probe experimental setup for the Rayleigh-scattering measurements. Intensity of the Rayleigh scattering as the function of the pumping energy in two different dye-Ag aggregate mixtures. Lower inset: 1 – spectrum of scattered light and spontaneous emission, 2 – spectrum of spontaneous emission only.

The scattered probe light was seen in the spectrum as a relatively narrow (~ 5 nm) line on the top of a much broader spontaneous emission band (Fig. 3 lower inset) and could be easily separated from the spontaneous emission. The six-fold increase of the Rayleigh scattering observed in the dye-Ag aggregate mixture with the increase of the pumping energy (Fig. 3, squares) is the clear experimental demonstration of the compensation of loss in metal and enhancement of the quality factor of surface plasmon resonance by optical gain in a surrounding dielectric. This is an appropriate point to introduce a measurement system for control by gain or loss through the method called ATR, which was briefly referred to above.

3.2. Compensation of loss in propagating surface plasmon–polaritons by optical gain

The famous attenuated total internal reflection (ATR) system [61] has the typical experimental arrangement shown in Fig. 4. The pumping permits the introduction of gain, and because it is an ATR device, it deploys a glass prism that has a dielectric permittivity $\varepsilon_0 = n_0^2$, a metallic film with the complex dielectric constant ε_1 (medium 1) and thickness d_1. The usual ATR system is extended, here, with the addition of a gain medium dielectric layer characterized by the complex relative permittivity $\varepsilon_2 = \varepsilon_2^{'} + i\varepsilon_2^{''}$ (medium 2), made *active* by pumping in the manner shown in Fig. 4.

A surface plasmon–polariton created at the boundary between medium 1 and 2 has a wave vector [60, 61]

$$k_x^0 = \frac{\omega}{c}\sqrt{\frac{\varepsilon_1\varepsilon_2}{\varepsilon_1+\varepsilon_2}}, \qquad (1)$$

where ω is the oscillation frequency and c is the speed of light. A surface plasmon–polariton is excited by p-polarized light incident through the prism upon the metallic film at an angle θ_0, greater than the critical angle for total internal reflection. The projection of its wave vector onto the x-axis is

$$k_x(\theta) = (\omega/c)n_0 \sin\theta_0 . \qquad (2)$$

This is a resonant condition, and the energy of the incident probe beam is transferred to the surface plasmon–polariton. This creates a minimum in the reflectance $R(\theta)$ [60, 61], where

$$R(\theta) = \left| \frac{r_{01}^{+} r_{12} \exp(2ik_{z1}d_1)}{1 + r_{01} r_{12} \exp(2ik_{z1}d_1)} \right|^2 , \qquad (3)$$

where $r_{ik} = (k_{zi}\varepsilon_k - k_{zk}\varepsilon_i)/(k_{zi}\varepsilon_k + k_{zk}\varepsilon_i)$ and

$$k_{zi} = \pm\sqrt{\varepsilon_i \left(\frac{\omega}{c}\right)^2 - k_x(\theta)^2}, \quad i = 0, 1, 2. \qquad (4)$$

The quantity $k_z c/\omega$ defines the field distribution along the z-direction. Its real part can be associated with a tilt of phase fronts of the propagating waves [67], while its imaginary part defines the wave attenuation, or growth.

The angular reflectance profile $R(\theta)$, Eq. (3), features a nearly Lorentzian "dip", for which the width is determined by the sum of internal (absorption), γ_i, and radiative, γ_r, losses [25, 60]. In *thick* metallic films (where $\gamma_i > \gamma_r$ in the absence of gain) the "dip" in the reflectance profile becomes deeper when gain is first added to the system, reaching its minimal value $R_{\min} = 0$ at $\gamma_i \approx \gamma_r$ [25]. With a further increase of the gain, γ_i becomes smaller than γ_r, leading

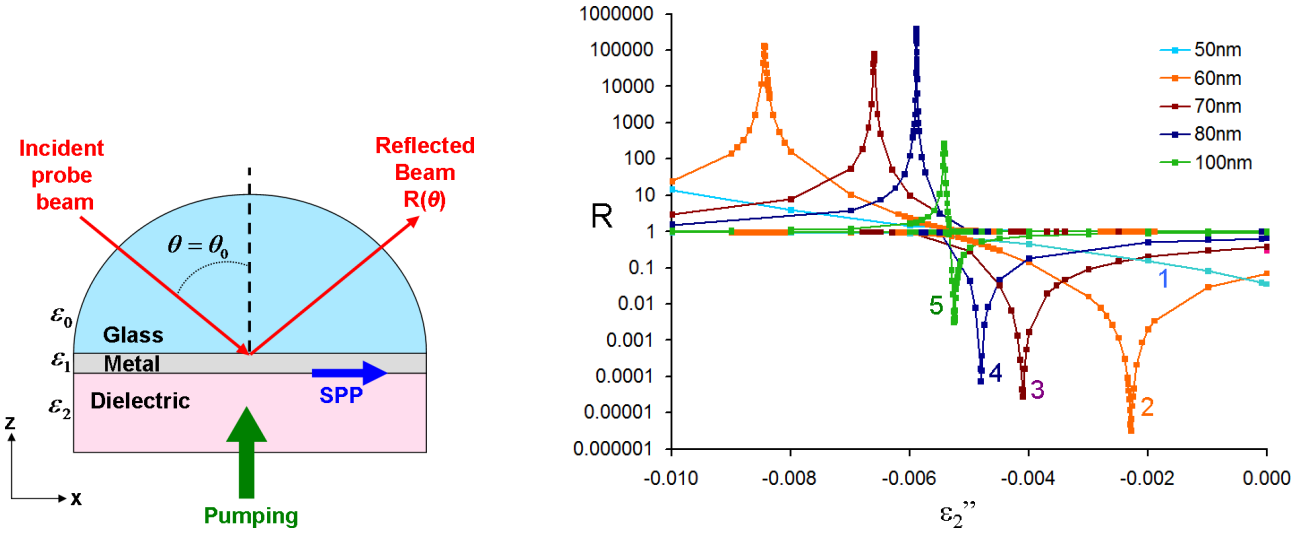

Figure 4 (online color at: www.lpr-journal.org) System to generate surface plasmon–polaritons. The figure shows the use of a hemispherical prism and surface waves are generated when the incident p-polarized probe beam exceeds the critical angle. The gain is introduced through an external electromagnetic beam that pumps the lower dielectric. Also shown, for different film thicknesses, is the dependence of the minimum (maximum) reflectance of the dip (peak) of the reflectance profile $R(\theta)$ versus ε_2''. The system parameters are $\varepsilon_0' = n_0^2 = 1.784^2 = 3.183$, $\varepsilon_0'' = 0$, $\varepsilon_1' = -15$, $\varepsilon_1'' = 0.85$, $d_1 = 39\,\text{nm}$, $\varepsilon_2' = n_2^2 = 1.5^2 = 2.25$.

to an increase of $R_{\min}$. This is the starting point for *thin* metallic films in which $\gamma_I < \gamma_r$ at $\varepsilon_2'' = 0$ and the resonant value of R monotonically grows with the increase of gain.

The resonant value of R is equal to unity when *internal* loss is completely compensated by gain ($\gamma_i = 0$) at $\varepsilon_2'' = -\frac{\varepsilon_1''\varepsilon_2'^2}{\varepsilon_1'^2}$ [25]. When gain is increased to even higher values, γ_i becomes negative and the dip in the reflectance profile changes to a peak. The peak has a singularity when the gain compensates *total* SPP loss ($\gamma_i + \gamma_r = 0$), as seen in the upper right inset of Fig. 4a. Beyond the singularity point, the system becomes unstable [68].

The minimum, or maximum, values of $R(\theta)$ are plotted versus ε_2'' for different thickness of the metallic film in Fig. 4a, and the corresponding values of the full width at half-maximum (FWHM) of a dip or a peak are depicted in Fig. 4b.

In Fig. 4, a glass prism is used with a refraction index $n_0 = 1.784$. Metallic films are created by evaporating pure silver. The gain material is rhodamine 6G dye (R6G) and polymethyl methacrylate (PMMA), dissolved in dichloromethane and deposited onto the surface of the silver and dried to form a film. The concentration of dye is 10 g/l (2.1×10^{-2} M) and the thickness of the polymer film is of the order of 10 µm.

The R6G/PMMA film is pumped in the manner shown in Fig. 4, with Q-switched pulses of a frequency-doubled Nd:YAG laser.

The results of the reflectance measurements for a 39-nm silver film are summarized in Fig. 5. Two sets of data points correspond to the reflectance without pumping (measured in flat parts of the kinetics before the laser pulse) and with pumping. By dividing the values of R measured in the presence of gain by those without gain, the relative

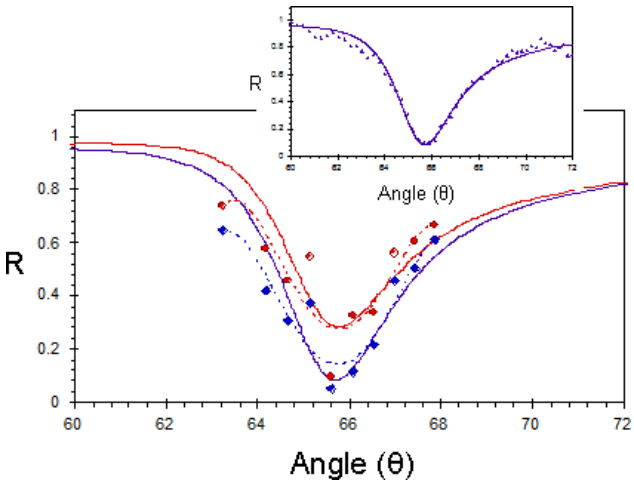

Figure 5 (online color at: www.lpr-journal.org) Reflectance $R(\theta)$ measured without (diamonds) and with (circles) optical pumping in the glass-silver-R6G/PMMA structure. Dashed lines – guides for the eye. Solid lines – fitting with Eq. (3) at $\varepsilon_0' = n_0^2 = 1.784^2 = 3.183$, $\varepsilon_0'' = 0$, $\varepsilon_1' = -15$, $\varepsilon_1'' = 0.85$, $d_1 = 39\,\text{nm}$, $\varepsilon_2' = n_2^2 = 1.5^2 = 2.25$, $\varepsilon_2'' \approx 0$ (blue) and $\varepsilon_2'' \approx -0.006$ (red). Inset: Reflectance $R(\theta)$ recorded in the same system without pumping (dots) and its fitting with Eq. (3) (solid line).

enhancement of the reflectance signal is calculated to be as high as 280% – a significant improvement in comparison to [69], where the change of the reflectance in the presence of gain did not exceed 0.001%. Fitting both reflectance curves with Eq. (3) and known $\varepsilon n_1 = -15$, $\varepsilon i_1 = 0.85$ and $\varepsilon_2' = n_2^2 = 2.25$, yields $\varepsilon_2'' \approx -0.006$. This corresponds to the optical gain of $420\,\text{cm}^{-1}$ (at $\lambda = 594\,\text{nm}$) and $\sim 35\%$ reduction in internal SPP loss.

There is a possibility of stimulated emission of surface plasmon–polaritons using R6G/PMMA films that are the order of 39 nm–81 nm in thickness, which allows stronger pumping of dye molecules in a layer adjacent to the silver surface. Optically pumped dye molecules in the vicinity of the silver film partly emit to the surface plasmon–polariton modes. The SPPs excited by luminescent molecules (reported earlier in [70, 71]) get decoupled from the prism at the angles corresponding to the SPPs' wave numbers.

The character of SPP emission excited via optically pumped dye molecules changes dramatically at high pumping intensity, i. e. the emission spectra is considerably narrower in comparison to those at low pumping, the narrowed emission spectra became almost independent of the observation angle, the dependence of the emission intensity is strongly nonlinear with a distinct threshold and, finally, the value of the threshold depends upon the observation angle θ.

Although nonlinear dependence of the SPP intensity on the pumping intensity and the narrowing of the emission spectrum are expected even below threshold, a good agreement between the theoretical and the experimental results serves as strong evidence that the observed emission is due to stimulated emission of SPPs in a regime when the total gain in the system exceeds the total loss.

Photonic metamaterials rapidly go into a plasmonic metamaterial regime but, as shown here, absorption in metal, which causes damping of localized surface plasmons and *propagating* surface plasmon polaritons, can be conquered by optical gain in the form of a dielectric medium adjacent to a metallic surface, or nanostructure. These results are exciting and pave the way to numerous applications of nanoplasmonics and metamaterials.

The previous sections have discussed the addition of gain, mainly in linear regimes, but the question of stability has not been addressed up to this point. The next section takes up this issue, basing its approach on well-established plasma-physics outcomes.

4. Linear gain and instabilities

In this section the concepts surrounding linear active media, constructed as metamaterials will be considered. To begin with, it should be emphasized that the metaparticles for which a metamaterial is the averaged entity become active, when loaded with certain devices, such as diodes and transistors. This procedure should lead to linear amplification/compensation of losses [17, 18, 72, 73]. Stability [35–37, 74, 75] may, then, be an issue, however, and for active media it must always be searched for. If the amplitude of a wave becomes large enough, for example, the active devices, embedded into the metaparticles, enter into the regime of saturation, or some sort of nonlinear instability will develop. In addition to investigating the regimes with linear spatial amplification, it is also necessary to work out how to suppress the generation of absolute instability.

4.1. Convective and absolute instabilities and requirements for spatial amplification conditions

As is well known from communication systems, such as ordinary radio/TV transmission systems, or radar systems, there are two main devices transforming the energy of an applied external electric field into electromagnetic oscillations, or waves. these are *generators* and *amplifiers*. Two types of instabilities may emerge, called *absolute* and *convective*, respectively, and correspond to two linear regimes: generation and amplification. In the absolute case, the field grows with time at any point in space, while in the convective case, the pulse/beam amplitude increases in space along the direction of propagation, as sketched in Fig. 6. These two types of instabilities can be associated with complex frequency, or wave number, respectively. To get spatial amplification, a system should possess a convective instability.

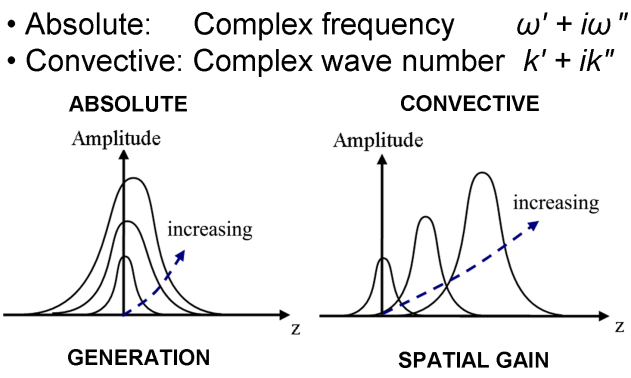

Figure 6 (online color at: www.lpr-journal.org) Interpretation of the absolute and convective instabilities using complex frequency $(\omega' + i\omega'')$ and wave number $(k' + ik'')$, respectively.

Avoidance of the absolute instability regime has been enunciated very clearly for small wave numbers, but the stability behavior at large wave numbers has only approximately been discussed in [17]. This outcome has its origin in a perceived problem connected with large wave number behavior, because the effective wavelength begins to assume a size that is the order of the metamaterial unit-cell dimension. In this review, this difficulty is overcome by engaging in transmission-line modeling [76]. This is in line with the fact that a concept of "analogous nanoparticle transmission lines" is becoming important now at optical frequencies [34]. The analysis of electromagnetic waves going through an unbounded, lossy, or amplifying, metamaterial leads naturally to a dispersion equation. How gain is created will not be discussed, at this stage of the argument, but placing Gunn, tunnel, or some other type of diode [75, 77–79] across the gap in the split-ring-resonator component of a typical metamaterial, for example, may be enough to achieve this property. The diodes must be biased to force them to have a negative resistance response, as shown in Fig. 7.

The behavior of a loss/gain system is quantified, in general, by a complex frequency ω related to a complex wave number $k = (0,0,k)$. Some mapping of ω onto the complex **k**-plane is required in order to work out what stability limits

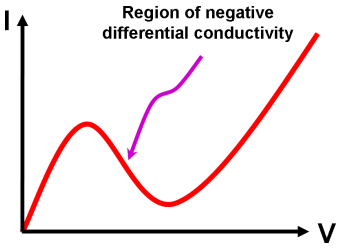

Figure 7 (online color at: www.lpr-journal.org) Example of current-voltage characteristic with negative differential conductivity in the case of tunnel diodes [75, 80].

a material may possess, so that some basic rules concerning absolute instability can be identified [35–37, 74, 75]. The definition of k given here, implies propagation along the z-axis and this wave vector component can be defined as the complex number $k = k' + ik''$. The complex frequency will be defined as $\omega = \omega' + i\omega''$. A typical wave, for the example being developed here, has the form $e^{i(\omega t - kz)}$, where t represents time. A typical set of mappings involving complex k and complex ω are shown in Fig. 8. The technique is to locate the roots of the dispersion equation on the complex k-plane, and then choose the real part of the frequency, and look at the paths traced out by the roots on the complex k-plane as the imaginary part of the frequency is varied. For the existence of absolute instability, a saddle point must exist, and a double root is reached for which $\omega'' < 0$. Indeed, the roots of the dispersion equation approach the saddle point from different halves of the complex k-plane. In fact, writing k_+ for $z > 0$ behavior, and k_- for $z < 0$ behavior means that $k_+ = k_-$ reveals the existence of a resonance implying a divergent growth without the necessity of a source.

Figure 8 shows what could happen to the complex k root locations as the upper and lower halves of the complex wave number plane is traversed. Specific details of the system are not given because they are not required at this stage. As ω? is varied, two roots approach each other [35] and a saddle point forms in the complex (k', k'') plane. The argument up to now involves a single plane wave but, in a real situation, a wave packet would be entered into a metamaterial. A plane wave is just a constituent of such a packet and will yield information on whether the packet will spread out, or not. A wave packet may grow everywhere in space and this can be caused by noise, or some other form of perturbation. If this happens then absolute instability is said to be created. It could be the case that the packet is being swept through the metamaterial very rapidly so that, at each point, the perturbation simply dies away at large times. This is more like the idea of an amplifying wave sweeping its way through the system and is called a convective instability. As is often pointed out, what actually happens is frame dependent so that what is absolute in one frame will be convective in another frame. Nevertheless, as Lifshitz and Pitaevskii [35] point out "there is always a preferred frame in an experiment" (sic), so instability is still a very important question no matter what frame any experiment is performed within. In the example to be given in the next section, such a saddle point is identified, and it occurs at $k = 0$, i. e. at a zero of the dispersion equation. Besides this, there is an essential singularity associated with the $|k| \to \infty$ pole of the dispersion equation [35]. It is important, therefore, to determine both the $k = 0$ roots *and* the $|k| \to \infty$ poles of the dispersion equation yielded by split-ring-resonator/wire types of metamaterial.

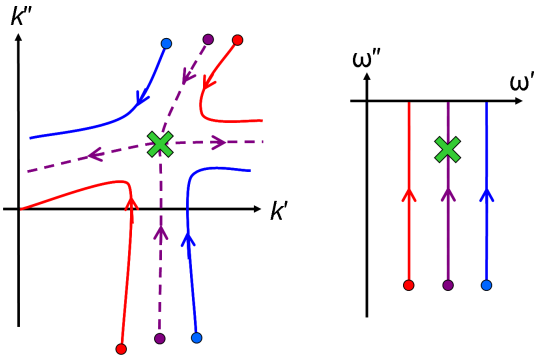

Figure 8 (online color at: www.lpr-journal.org) An example of outcomes of the mapping of the complex ω-plane, where $\omega = \omega' + i\omega''$, onto the complex k-plane, where $k = k' + ik''$. A saddle-point is designated by the cross. The are the starting points of the contours.

Materials based on a regular (periodical) structure of metaparticles will be considered here. As follows from the analysis of absolute instability, a number of possibilities for such an instability occur for periodic systems. In practice, a beam may be entered into the system that has a limited extension, say, along the x-axis. In Fourier space, therefore, such a beam covers all the wave number range from $k = 0$ to $k = \infty$ including wave numbers corresponding to the fundamental resonance of a periodic system, for which $kd = \pm\pi$, where d is the spatial period. These are special points in k space, leading to absolute instability. Unfortunately, beam propagation is associated with Fourier components in the tails of the spectrum and access both resonance ($kd = \pm\pi$) and $|k| = \infty$ regions. Instability connected with the pole of the dispersion equation [35] can also be created, when $|k''|$ becomes very large, while $|k'|$ is finite, where k', k'' are, respectively, real and imaginary parts of the wave number. Therefore, the instabilities discussed above have to be taken into account. Note also that even for a small amplitude of the Fourier component of a beam, in the range of intrinsic resonance of the system, namely, $kd = \pm\pi$, absolute instability can develop, if the system is used for a linear spatial amplification of a beam for a long enough time.

A sketch of the three main types of possible special points that determine the type of instability is shown in Fig. 9.

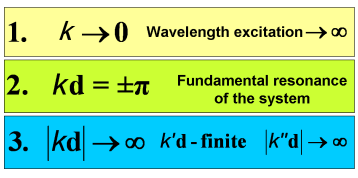

Figure 9 (online color at: www.lpr-journal.org) Possible types of absolute instability in a periodic system with period d.

The task now is to find a nice presentation of these instability points and to find a means of suppressing them. In order to do this, an analysis will be developed of a trans-

mission line, because this permits the selection of all three kinds of instability points.

4.2. Active elements/active media characteristics

One of the concepts employed here, is that the creation of stable gain for electromagnetic waves propagating through an active metamaterial, needs a frequency-dependent conductance $g(\omega)$, where ω is an arbitrary, possibly complex, frequency. The discussion here is restricted to nongyrotropic and reciprocal media, so it is possible to use the most popular amplifying devices, such as supercritical Gunn diodes, or transistors, that may lead to an absolute instability. Instead, subcritical Gunn diodes [79, 81–83] are used. The natural result is a lower output power and efficiency compared to supercritical diodes [82], but, nevertheless, they can provide spatial gain and convective instability and therefore an absence of absolute instability [35, 36, 79, 81, 83] for active metamaterials. The point is that if the "host media", a transmission line, in this case, does not possess the property of nonreciprocity [1, 36], so the condition for the absence of absolute instability can be fulfilled with subcritical diodes that do not have "intrinsic instability". The latter shows itself as spontaneous oscillations in the circuit that include only diode and load resistance, and in particular, in the limit of zero resistance [79, 81, 82]. It is possible to show that, qualitatively, this requirement corresponds to the frequency dependence of a complex diode conductivity, having the form

$$g(\omega) \equiv g_0 \mathrm{e}^{\mathrm{i}\varphi} / \{1 + \mathrm{i}[(\omega^2 - \omega_0^2)/(\omega\Delta\omega)]\}, \quad (5)$$
$$g_0 < 0, \quad g'(\omega) = \mathrm{Re}(g(\omega)), \quad g''(\omega) = \mathrm{Im}(g(\omega)),$$
$$-\pi < \varphi < \pi,$$

where $\Delta\omega$ is a bandwidth, ω_0 is a constant and $g'(\omega)$ and $g''(\omega)$ are real and imaginary parts of conductance, respectively. The phase value $\varphi = \pi$ is excluded, to preserve the negativity (in some frequency range) of the real part of the conductivity. A detailed search for possible stability/instability will now be presented. The denominator of $g(\omega)$ vanishes whenever

$$\omega = \frac{\mathrm{i}\Delta\omega \pm \sqrt{4\omega_0^2 - \Delta\omega^2}}{2} \quad (6)$$

and the imaginary parts are positive, for small enough $\Delta\omega$. This provides for the absence of absolute instability, connected with such "special" points. The phase value $\varphi = 0$ corresponds to the coincidence of the frequency points associated with a change of sign of the imaginary part of conductivity and maximum of an absolute value of its real part [79]. Note that the case $\varphi = -\pi/2$ corresponds qualitatively to the resonant behavior of $g(\omega)$ described by the model of subcritical diode presented in [77]. If $\varphi = -\pi/2$ then, from Eq. (5), the real and imaginary parts of the conductivity become

$$\mathrm{Re}(g(\omega)) \equiv g'(\omega) = -g_0 \frac{\left[\left(\omega^2 - \omega_0^2\right)/(\omega\Delta\omega)\right]}{\left\{1 + \left[\left(\omega^2 - \omega_0^2\right)/(\omega\Delta\omega)\right]^2\right\}}, \quad (7)$$

$$\mathrm{Im}(g(\omega)) \equiv g''(\omega) = -g_0 \Big/ \left\{1 + \left[\left(\omega^2 - \omega_0^2\right)/(\omega\Delta\omega)\right]^2\right\}. \quad (8)$$

In this case, $|g(\omega)'|$ has a maximum equal to $|g_0|/2$ at the (real) frequency

$$\omega = \omega'_{\max} \approx \omega_0 - \frac{\Delta\omega}{2}, \quad (9)$$

if $\Delta\omega \ll \omega_0$ $\Delta\omega$ determines the effective frequency bandwidth, where $g(\omega)' < 0$ and gain may be possible. Hence, the main result for the consideration of instability for metamaterials with active metaparticles, loaded with active elements, with conductivities described by dependences in the form of Eqs. (7) and (8) is the exciting possibility of overcoming absolute instability and the creation of an active metamaterial, where the spatial gain is possible.

4.3. Modeling linear active metamaterial

A type of transmission line that gives a dispersion characteristic analogous to that of metamaterials based on split-ring resonator is proposed in [12], and we use the equivalent circuit of the same type here, as shown in Fig. 10. The interpretation of the elements of the equivalent circuit is explained in the caption to Fig. 10. The question of where to introduce the active element (diode) into the transmission-line cell is not a straightforward one to answer. A choice has been made here, however, by adding it in parallel with C_r, R and L_r: thus placing it in the resonant part of the circuit. The form of $g(\omega)$ selected corresponds to the Eqs. (7) and (8).

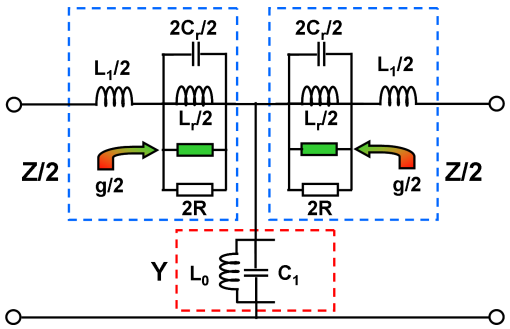

Figure 10 (online color at: www.lpr-journal.org) Equivalent (symmetric) T-circuit representing the unit cell of a 1D transmission-line with a width (period) d, and loaded with an active diode. C_r, L_r, R are the equivalent components to those that describe the split-ring resonator. L_1, C_1, L_0 account for the dielectric background and the wires. The unit cell operates in the transmission line as a frequency-dependent impedance, $Z(\omega)$ and an admittance, $Y(\omega)$.

The imaginary part of diode conductivity could include also a specific "static" capacitive component [79, 84], but it can be included into the element C_r of the equivalent circuit in Fig. 7 and not considered here. The time and space variation assumed here is $\exp(\mathrm{i}[\omega t - kz])$, where z points along the transmission-line This type of frequency dependence could be provided, if necessary, with a dedicated external circuit. $Z(\omega)/2$, the *impedance* of each of the symmetric horizontal parts of the T-circuit, is determined by the elements $L_1/2, C_r/2, L_r/2, 2R_r, g(\omega)/2$. $Y(\omega)$, the *admittance* of the vertical part of the T-circuit, is determined by the elements L_0, C_1. In fact, as can be appreciated from a transmission-line representation of free space, Z (the impedance) and Y (the admittance), for any transmission line, are proportional to the effective magnetic permeability and effective dielectric permittivity, respectively.

For the transmission line T-circuit, shown in Fig. 10, since the value of d is finite, the dispersion equation is

$$F(\omega,k) = \cos(kd) - 1 - YZ/2 = 0. \qquad (10)$$

Note that in the longwave regime, $kd << 1$, and this corresponds to the standard form for the metamaterials approximation of continuous media, the dispersion equation then becomes

$$(kd)^2 = -YZ. \qquad (11)$$

As discussed in Section 4.2, possible sources of absolute instability, are the saddle (bifurcation) points in the complex-wave-number plane and the essential singularities $k \to \infty$ (poles) in either of the dispersion equations given by Eqs. (10) and (11). The discussion of how to locate possible instabilities will now be given, briefly, below, but it is worth commenting upon the specific condition $k \to \infty$, because this seems to be impossible to reach, in a real system. The condition $|k| \sim \frac{1}{d}$ is a reasonable restriction, at this stage, for $|k|$. Nevertheless, determining the possibility of the existence of "poles" in the dispersion equation will yield qualitative and quantitative information about the possible onset of absolute instability before this physical transition to short-wavelength behavior occurs. Consider now the "special points", connected with possible instabilities, including "saddle points" and "poles".

4.3.1. Saddle points

These points occur in the complex wave number plane in which $k = k' + \mathrm{i}k''$ and, in general, for complex frequency, whenever,

$$F(\omega,k) = 0, \quad \partial F/\partial k = 0, \qquad (12)$$

from which emerge the roots $kd = 0$, $Y(\omega)Z(\omega) = 0$ and $kd = -\pi$, $Y(\omega)Z(\omega) = -4$. It is interesting that this regime is defined by $k' < 0$ with a positive group velocity, i. e. negative-phase behavior. The complex roots ω of these equations yield the "special (absolute instability) points" from the sign of their imaginary parts, while $\omega'' \equiv \mathrm{Im}(\omega) < 0$ corresponds to the presence of absolute instability [35, 36]. Hence, the branch points in the complex frequency plane are locatable.

4.3.2. Poles of the dispersion equation

The large wave number limit corresponds to poles of $k(\omega)$ and, therefore, to poles of $Y(\omega)$ and $Z(\omega)$. They can be found in a straightforward way from an analysis of the lumped elements displayed in the circuit shown in Fig. 10.

Using the equivalent circuit shown in the Fig. 10, it is possible to show that each of the expressions for $Y(\omega), Z(\omega)$ could be presented as a ratio of polynomials. The pole of Y corresponds to $\omega = 0$, where the effective conductivity is positive and does not lead to absolute instability. To avoid absolute instability, it is necessary to find locations of the roots of the polynomials in the ratio defined by $Z(\omega)$. All the roots must lie in the upper half-plane of "complex ω" [35–37, 74]. This applies not only to the numerator, but also to the denominator of the expression for $Z(\omega)$, because poles, corresponding to $|k| \to \infty$ could also be sources of absolute instability [35]. Instead of using laborious methods of direct investigations of the polynomials roots [18, 85], we apply here the method of perturbations that is valid, in particular, for $\varphi = -\pi/2$ and $g(\omega)$ is taken in the form of Eqs. (7) and (8) in the case

$$\frac{\omega_0 L_r}{R} \sim \omega_0 L_r |g_0| \ll \frac{\Delta\omega}{\omega_r} \ll 1, \quad \omega_r = \frac{1}{\sqrt{L_r C_r}}. \qquad (13)$$

Analysis of the saddle points (see Eqs. (12)) and large complex wave number ($|k| \to \infty$) (poles) imposes the condition upon the diode conductance necessary for the absence of absolute instability and presence of gain, namely

$$\begin{gathered} 1/R(1+S_*) < (-g_0) < (1+S)(1/R), \\ S = \min\left(S_{\mathrm{saddle}}, S_{\mathrm{pole}}\right). \end{gathered} \qquad (14)$$

The values S_{pole}, S_{saddle} and S_* are not presented in detail here. S_{pole} and S_{saddle} correspond to the poles of $k(\omega)$ and the saddle points of the dispersion function $F(\omega,k)$, respectively. Note that special points connected with poles of $g(\omega)$ do not lead to absolute instability. This is possible to show using Eqs. (6), (7)(7), (8) and (13). The right-hand side of the inequality (14) determines a condition of absence of absolute instability, while the left-hand side of this inequality (including the value S_*) determines the possibility of amplification, at least at the frequency $\omega'_{\max}$, where $|g(\omega)'|$ reaches its maximum value.

Previous analytical results are obtained for the particular media described by the equivalent circuit shown in Fig. 10 and conductivity in the form of Eqs. (7)(7) and (8) (with $\varphi = -\pi/2$). Consider a metamaterial described by the equivalent circuit shown in Fig. 10 with a conductivity belonging to a rather wide family described by Eq. (5) (with $-\pi < \varphi < \pi$). The discrete sets of all special points, including saddle points of the dispersion function, and poles, namely $\omega_{1\mathrm{rt}}, \omega_{2\mathrm{rt}}, \ldots, \omega_{n_{\mathrm{saddle}}}$ and $\omega_{1\mathrm{pole}}, \omega_{2\mathrm{pole}}, \ldots, \omega_{n_{\mathrm{pole}}}$, respectively, which are assumed to be close to the axis $\mathrm{Re}\,\omega$. This is the case, when conditions similar to Eq. (13) are satisfied and losses/gain are small enough. Here n_{saddle}, n_{pole} are total numbers of roots (saddle points) and poles, respectively. Once these are determined, then an ordered unification of

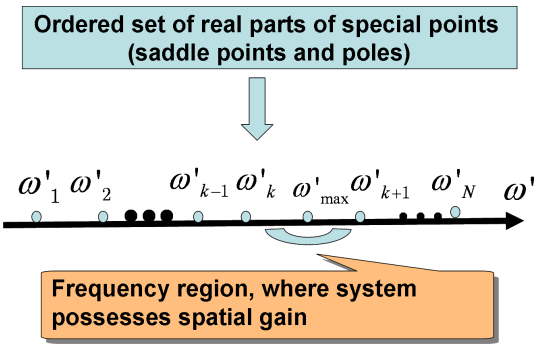

Figure 11 (online color at: www.lpr-journal.org) Ordered set of special points (saddle points of dispersion function (Eq. (12)) and poles of wave number) and region of frequencies (denoted by the arc), where the system is active (spatial amplification is present). It is supposed that losses/gain are small enough, the method of perturbation is valid, and that all special (frequency) points are lying close to the real axis of the complex frequency plane. By means of a proper choice of parameters (such as ω_0 and $\Delta\omega$), provision of the frequency $\omega_{\max}^{'}$ is assumed (corresponding to the maximum of the absolute value of real part of the conductivity $g(\omega)$) and the whole frequency interval (shown by the arc), where spatial amplification is present, belongs to the range of negative-phase behavior.

the two sets, namely, $\omega_1', \omega_2', \ldots, \omega_{k-1}', \omega_k', \omega_{k+1}', \omega_N'$, where $N = n_{\text{saddle}} + n_{\text{pole}}$ (Fig. 11) can be constructed. Any special point connected with the pole of $g(\omega)$ should have positive imaginary part (see, for example, Eq. (6)), and in this case, absolute instability would not be connected with such a special point. Therefore this type of special point is excluded from further consideration and the constructed set of points ω_l', $l = 1, \ldots, N$. Suppose that frequency, corresponding to a maximum value of the (negative) real part of diode conductivity $g(\omega)'$, is $\omega_{\max}^{'}$. The frequency $\omega_{\max}'$ can be located either to the "left", to the first frequency point of the set of special points, $\omega_{\max}' < \omega_1^{'}$, or to the "right", to the last point of this set, $\omega_{\max}' > \omega_N^{'}$, or between two neighboring frequency points ω_k' and ω_{k+1}', belonging to this set. Consider the case $\omega_k' < \omega_{\max}^{'} < \omega_{k+1}'$ (the result is qualitatively the same also for other possible cases of location of $\omega_{\max}^{'}$). Even if a more general equivalent circuit is used than that shown in Fig. 10, it is always possible to connect some resistance R, for example, in parallel with the conductively of the active element, to control its "effective conductivity" $g'(\omega') + \frac{1}{R}$. The (finite) bandwidth $\Delta\omega$, conductivity g_0 and resistance R can be selected in such a way, that the value $g'(\omega') + \frac{1}{R}$ is negative only in the range of frequency, centered at $\omega_{\max}'$, denoted by the arc in Fig. 11, and lying entirely inside an interval $(\omega_k', \omega_{k+1}')$.

Suppose also that the frequency $\omega_{\max}^{'}$ and the frequency interval (shown by the arc in Fig. 11), where the "effective conductivity" of the active element together with the parallel resistance is negative, are located inside the range of negative-phase behavior. This can be provided easily by means of proper choice of parameters, such as ω_0 and $\Delta\omega$.

At the same time, it is possible to show, in the framework of applicability of this perturbation method, that the imaginary parts of the set of special points are proportional to the corresponding values of "effective conductivities" and are positive, $\omega_l'' \sim (g'(\omega_l^{'}) + \frac{1}{R_r}) > 0$, $l = 1, \ldots, N$. These values are positive because, as was noted previously, for chosen parameters, all "special points" lie close to the axis of "real ω" and outside the region, where "effective conductivity" is negative, shown by the arc in Fig. 11. The positivity of all ω_l'' provides an absence of absolute instability and therefore, a *possibility of spatial gain* [35, 36]. This is an important qualitative result. Note also that when the values of gain/losses are small enough, a presence of gain/losses *does not destroy "negative-phase behavior"*, at least in a narrow enough range of frequencies shown by the arc in Fig. 11. Therefore the media still also possesses the property of negative-phase behavior. In fact, in the present investigation, it required only the following rather general properties of the "host media" and active elements: (a) an active element must not possesses "intrinsic instability", in other words the pole of $g(\omega)$ has positive imaginary part, (b) $g(\omega)$ is negative only in a restricted range of frequencies, determined by some parameter $\Delta\omega$ (c) the set of saddle points and poles is discrete. (d) a smallness of loss/gain and applicability of the method of perturbation. (e) a range of frequencies exists with negative-phase behavior that is compatible with a spatial gain, and a proper choice of the parameters. The proposed approach based on the fulfillment of the conditions (a)–(e) of spatial amplification is qualitatively valid for a wide class of active media with negative-phase behavior, and the active metamaterial described by the equivalent circuit in Fig. 10 and Eqs. (7) and (8) is only one particular object, belonging to this class. This approach can be used not only for analysis, but even for a "construction" of new active metamaterials with negative-phase behavior.

Numerical results presented here are obtained for the media described by equivalent circuit shown in Fig. 10 with an active element, and the conductivity is described by Eqs. (7) and (8) (with $\varphi = -\pi/2$).

In Fig. 12 the ranges of normalized conductivity $G = |g_0|\omega_r L_r$, existing between lower and upper curves (corresponding to the left and right parts of the inequality (14), respectively) are shown as a dependence upon relative bandwidth $\Delta\omega/\omega_r$. The lower curve, determining this range, implies a minimal normalized conductivity $G = |g_0|\omega_r L_r$ that is necessary at least to compensate losses at the frequency point $\omega_{\max}'$, where the absolute value of the (negative) real part of the conductivity reaches its maximum. The upper curve determines the maximum possible value of conductivity $G = |g_0|\omega_r L_r$, which is still compatible with the condition of the absence of absolute instability. It is interesting to note that (under selected parameters) in the case $\varphi = -\pi/2$ a maximum possible value of $G(G_{\max}$, Fig. 12) is determined by the roots (branch point) corresponding to $k'd = -\pi$, while in the case $\varphi = 0$, the corresponding limit of G is determined by the root (branch point) $k'd = 0$.

In Fig. 13, the frequency dependences of the real and imaginary parts of the normalized wave number are shown,

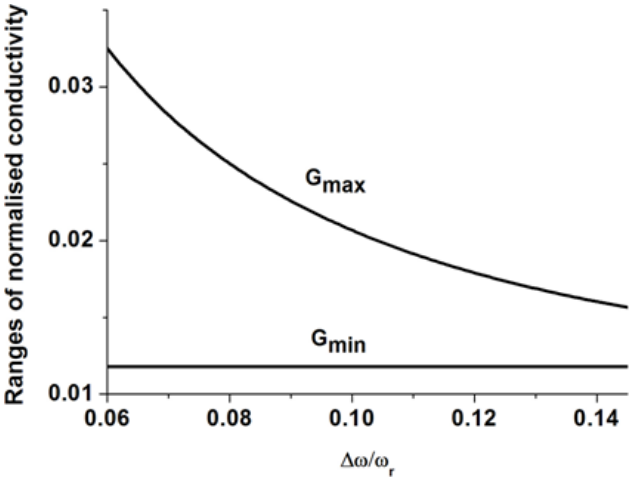

Figure 12 Ranges of normalized conductivity $G = |g_0|\omega_r L_r$ corresponding to the spatial amplification in dependence of relative bandwidth $\Delta\omega/\omega_r$ for the case $\varphi = -\pi/2$. Values $G_{\min}$ and $G_{\max}$ correspond to the left and right parts of the inequalities (16), respectively.

as a function of frequency, normalized with the value $\omega_r = 1/\sqrt{C_r L_r}$. The curves are generated using the circuit shown in Fig. 10 and the conductivity $g(\omega)$ defined earlier. Dispersion is computed using the method of perturbation, when relations (13) and the condition $|k'| \gg |k''|$ are valid.

A rather wide class of active media and a rather general approach for analysis and/or even "construction" of new such media is proposed here. For such media, a spatial amplification (with $k''d > 0$) is achievable in the range of negative-phase behaviors with $V_g V_{ph} < 0$, where V_g and V_{ph} are respective group and phase velocities of the electromagnetic waves in a metamaterial. An equivalent circuit based upon split rings is relevant to frequency windows that range well into the infrared. The concept of absolute and convective instability can also be extended to include optical frequencies.

The paper now turns towards some particular forms of amplification, nonlinearity and system tunability. The first involves a superheterodyne method.

5. Superheterodyne amplification in active layered metamaterial structures in the THz or infrared frequency ranges

The principle of superheterodyne amplification is the parametric transformation of amplification from a lower to an upper frequency band, under the condition that some definite linear mechanism of amplification in the lower band exists. This principle was first proposed [86, 87], for amplification of acoustic waves in a piezosemiconductor and electromagnetic waves in active media, and for amplification of magnetostatic waves in ferrite layers [88]. It has been proposed [89, 90] that the transformation of a linear amplification of a space charge wave [42, 43] in n-GaAs film to an electromagnetic wave should take place through a (nonlinear) parametric mechanism. Either bulk n-GaAs or a two-dimensional electron gas can be used in a layered semiconductor structure. Superheterodyne amplification, therefore, can be applied, in principle, for electromagnetic waves in quantum metamaterials [91]. Here, it is proposed that an application of this principle be developed for the amplification of backward electromagnetic waves in metamaterials, in the THz or the IR ranges. The waveguide geometry is shown in Fig. 14.

In order to be specific, only electromagnetic waves in IR range will be considered. For this simplified consideration symmetrical layered structure of Fig. 14, with GaN-and metamaterial layers, it is assumed that the "GaN" layer has the same properties as n-GaN without any detailed consideration of the real geometry of GaN layer(s), which includes, in fact, a substrate and "active n-GaN".

Given that GaN is placed in the region $-l \leqslant x \leqslant l$, and that metamaterial occupies the regions $x > l$ and $x < -l$, antisymmetric electromagnetic modes are considered. A sta-

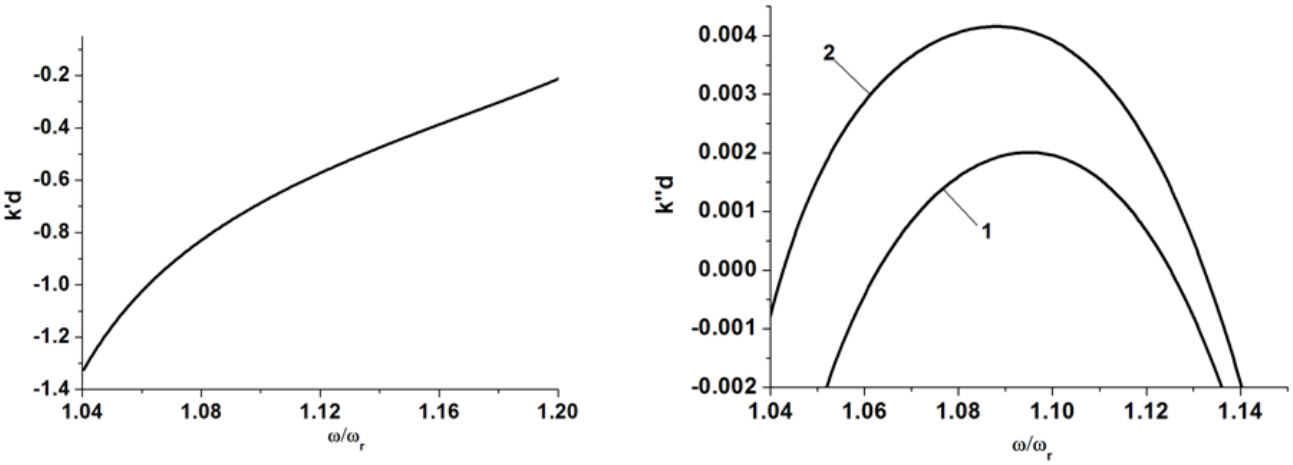

Figure 13 Dependences of real (a) and imaginary (b) parts of normalized wave number on normalized frequency ($\omega_r = 1/\sqrt{C_r L_r}$) for the case $\varphi = -\pi/2$; $\Delta\omega/\omega_r = 0.14$; $\omega_r L_r/R_r = 5.8 \times 10^{-3}$; curve 1 in Fig. 13b is built for. $g_0\omega_r L_r = 0.013$; curve 2 – for $g_0\omega_r L_r = 0.014$.

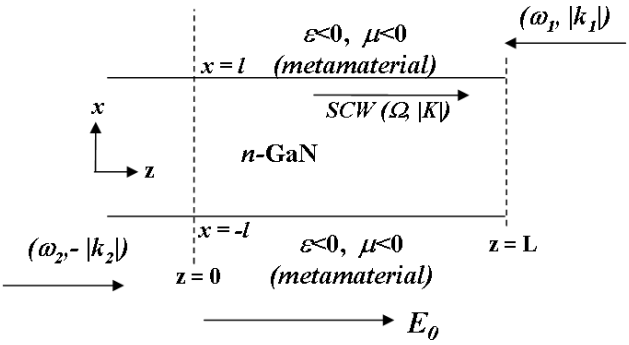

Figure 14 Geometry of superheterodyne amplification of electromagnetic waves interacting with a space charge wave (SCW) in a metamaterial/GaN/metamaterial structure. An amplified electromagnetic wave (signal) with frequency ω_2 is launched at $z = 0$, and an electromagnetic pump wave is launched with frequency $\omega_1 > \omega_2$ at $z = L$ (L is the length of the system). A SCW with frequency $\Omega = \omega_1 - \omega_2$ ($\Omega \ll \omega_{1,2}$) is excited in the system (up from the level of noise) due to parametric coupling. E_0 is an external constant applied electric field.

tionary (DC) electric field E_0 is the source of amplification in the GaN, in the negative differential conductivity region, and is directed along the z-axis. Data is adopted to model this near-infrared regime, which means choosing an operating frequency of the order of $\omega \sim 10^{15}\,\mathrm{s}^{-1}$. In addition, the values selected for the relative electric permittivity and relative magnetic permeability of the metamaterial(s) are $\varepsilon \sim -2$, $\mu \sim -0.2$, respectively. The data for the GaN layer are $\varepsilon_2 \approx 5$, $2l = 0.8\,\mu\mathrm{m}$. In such a system backward (with oppositely directed phase and group velocities) antisymmetric (relatively to the x axis) electromagnetic waves, with the TE(H)-wave components (H_x, E_y, H_z), can propagate. Also, an effective overlap of the transverse profiles of antisymmetric electromagnetic modes and space-charge waves is now possible.

The phase-matching conditions corresponding to Fig. 14 are

$$\omega_1 - \omega_2 = \Omega\,, \tag{15}$$

$$|k_1| + |k_2| = \mathrm{K}\,, \tag{16}$$

where $\omega_{1,2}$, $k_{1,2}$ are the frequencies and wave numbers of backward electromagnetic waves 1, 2, respectively and Ω, K are the frequency and wave number of the space-charge waves, under the conditions $\omega_1 > \omega_2 \gg \Omega$. The choice of signs in Eq. (16) corresponds to the directions of the corresponding wave vectors shown in Fig. 14, so that the wave numbers of the electromagnetic waves with smaller frequency (wave 2) and space-charge waves are codirectional, while wave numbers of electromagnetic waves 1 and 2 are contradirectional. Only the form of the coupled equations is presented here for the amplitudes of the electric fields of electromagnetic waves $(E_{1,2})$ and the concentration of space-charge waves (U), under the condition

$$\Omega \ll \omega_{1,2}\,. \tag{17}$$

Hence, the basic equations governing the whole process are

$$\frac{\partial \mathrm{E}_1}{\partial t} - |V_\mathrm{g}|\frac{\partial \mathrm{E}_1}{\partial z} = -\beta_\mathrm{e}\mathrm{E}_2 U - \alpha_\mathrm{e}\mathrm{E}_1\,, \tag{18}$$

$$\frac{\partial \mathrm{E}_2}{\partial t} + |V_\mathrm{g}|\frac{\partial \mathrm{E}_2}{\partial z} = \beta_\mathrm{e}\mathrm{E}_1 U^* - \alpha_\mathrm{e}\mathrm{E}_2\,, \tag{19}$$

$$\frac{\partial U}{\partial t} + V_{\frac{\partial U}{\partial z}} = \beta_\mathrm{u}\mathrm{E}_1\mathrm{E}_2^* + \alpha_\mathrm{U} U\,, \tag{20}$$

with coupling coefficients β_e, β_u, loss coefficient α_e and linear gain $\alpha_\mathrm{U} > 0$. The value of α_U is proportional to the absolute value of negative differential conductivity of a semiconductor [89, 90] (n-GaN in the case under consideration).

Without entering into detailed calculations, it can be concluded that there is an important difference between possible mechanisms of amplification in positive-phase and negative-phase media. In positive-phase media [89], the superheterodyne mechanism implies that the electromagnetic wave 2, with lower frequency, is a pumping wave (with finite input amplitude), while the electromagnetic wave 1 (with larger frequency) is amplified. In this case, in the approximation of the *constant* pumping, an exponential dependence of amplified wave amplitude on the system length is obtained. In the negative-phase media, the situation changes markedly. Specifically, for negative-phase media, the optimum coefficient of amplification along with an exponential dependence of the amplitude of the amplified wave upon the system length is achieved when the pumping derives from electromagnetic wave 1, while the electromagnetic wave 2 with the smaller frequency, $\omega_2 \leqslant \omega_1$, is amplified. Using the conditions in Eq. (16) and the geometry in the Fig. 14, in this case, an amplified wave (2) is launched into the system at $z = 0$, while pumping wave is launched at $z = L$.

Evaluating the amplification of quasistationary space-charge waves in a thin GaN film, gives, for a carrier concentration in n-GaN of $n_0 = 2 \times 10^{17}\,\mathrm{cm}^{-3}$, and a thickness of the GaN film equal to $0.8\,\mu\mathrm{m}$, can be carried out using a constant electric field $E_0 = 150\,\mathrm{kV/cm}$, a maximum spatial increment for space-charge waves occurs at a frequency $f = \omega/(2\pi) \sim 200\,\mathrm{GHz}$ yielding approximately $k'' \sim 1.5 \times 10^4\,\mathrm{cm}^{-1}$. For $\omega_{1,2} \sim (0.5\text{–}1) \times 10^{15}\,\mathrm{s}^{-1}$, an effective amplification is of the order of magnitude ~ 100 can be achieved for an electromagnetic wave where $L \leqslant \sim 1\,\mathrm{mm}$ and using a pumping wave power $\sim 10\,\mathrm{MW/cm}^2$. Such a power is quite possible in a pulsed regime for GaN, in particular with a pulse duration less than 1 ns [92]. It is interesting, that, as has been previously shown [93], excitation of very high-frequency ($f = 30$–$200\,\mathrm{GHz}$) hypersonic waves is possible due to coupling with amplified space-charge waves of millimeter range in GaN films. This provides a perspective for applications in the field of high-frequency acoustic metamaterials. Finally, on the basis of these estimations it can be concluded that superheterodyne amplification of electromagnetic waves in the IR range in a layered system with layers of n-GaAs and metamaterials can be very effective.

A number of interesting linear scenarios for dealing with gain in metamaterials have now been given, together with an important stability analysis. It is appropriate at this point,

therefore, to examine nonlinear metamaterials in order to measure how active control can also be introduced into their manipulation.

6. Nonlinear and tunable metamaterials

The discussion up to now has not only centered upon linear metamaterials but has avoided a specific discussion of tunability. This section is designed to open up an investigation of these issues. Dynamic control tunability means deploying external features, or signals, designed to have accessible and adjustable characteristic properties. For example, could tunability in metamaterials be achieved through tailoring their electromagnetic properties to be dependent, specifically, on external optical, mechanical, electric or magnetic factors or control signals.

On the level of applications, on the other hand, tunable metamaterials offer unprecedented opportunities because a metamaterial structure, being artificial, can be designed with flexible designs that offer a strong degree of control for any intended operation.

A major step towards active and tunable metamaterials was made with some early research on *nonlinear metamaterials* [94, 95]. The relevance of these studies is driven by the numerous possibilities of exploiting the nonlinear processes for control of electromagnetic radiation, realization of tunable devices, harmonic generation and numerous applications [96]. The latter range from radio waves to the optical frequency window. The key is the insertion of nonlinear devices (diodes, for example) into a metaparticle [94], or using elements in nonlinear host media [95], accessing distinct nonlinear phenomena [18,27,97–101]. They often have a very important common feature, namely, nonlinearity connected with a field in a gap of metaparticles. For example, split-ring resonators show this feature very strongly under resonant conditions [23]. More recently, progress is being made towards electrically tunable, mid-infrared metamaterials [102]. The latter, once again, used split-ring resonators, but they are deposited upon doped indium antimonide, and the tuning is effected with the application of an external voltage to control the carrier density. Equally interesting, for the near-infrared, is the use of Ag split-ring resonators, patterned upon VO_2 [103]. The vanadium oxide enables frequency tuning from 1.5 μm all the way up to 5 μm.

Nonlinear metamaterials, however, open up a spectacular route to a wide variety of tunable and active metamaterials. The use of nonlinearity addresses quite different issues to the recent work on tuning that has just been discussed. In this case, tuning possibilities have been theoretically analysed for three-dimensional, nonlinear metamaterials [104], just based upon microwave implementation. However, since the general principles remain the same, provided that a qualitatively similar nonlinearity mechanism is accessible, scaling to higher frequencies is possible. A variable capacitance nonlinearity, for example, can be used for resonant frequency tuning (Fig. 15a), enabling efficient transition between transmission, reflection and absorption in the vicinity of resonance. On the other hand, variable resistance nonlinearity offers broadband transmission modulation through effective resistance modulation (Fig. 15b).

The first experimental advances involving a nonlinear approach to tunable metamaterials were reported for the microwave frequency range [44, 105–107], because it is much easier to implement the required design and assess the performance. All of this work shows that some very basic phenomena can be observed. The question is whether any real scaling to higher frequencies is possible.

One step forward towards this goal involves a split-ring resonator containing a varactor [106], and as will be seen below, a resonance frequency shift can be achieved that depends upon the energy of the electromagnetic radiation. This is a beautifully efficient means of actively controlling the transmission and reflection of a metamaterial [100]. Hence, nonlinear tunability opens up a way to efficient remote control over metamaterial properties.

In addition to the above, certain success has been achieved with a one-dimensional implementation of meta-

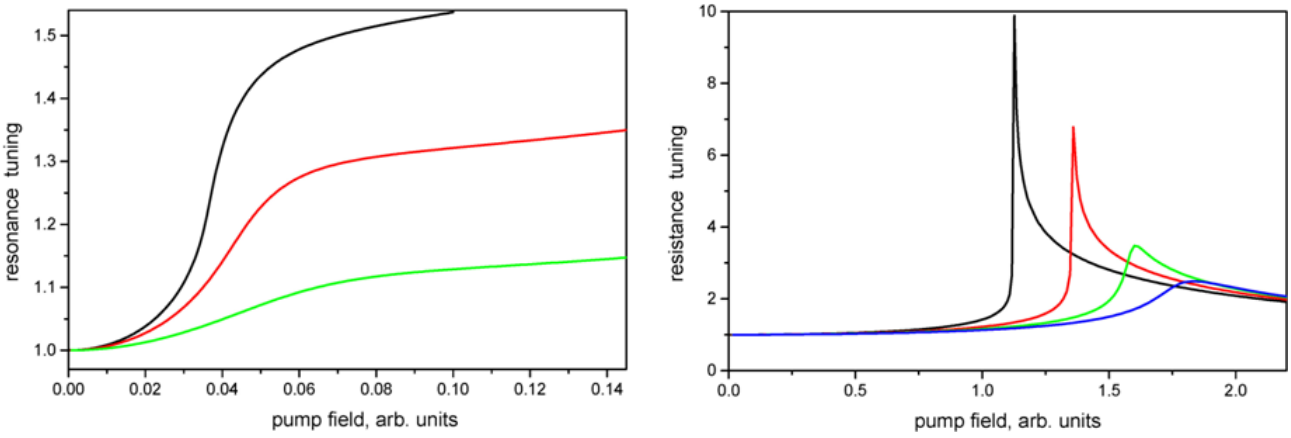

Figure 15 (online color at: www.lpr-journal.org) Tunability in nonlinear metamaterials provided with different types of nonlinearity, with variable capacitance insertions allowing for resonance frequency shift (left; shown for various varactor characteristics), and variable resistance insertions enabling extremely sensitive absorption tuning (right; shown for various backward diodes), as achieved with varying pump wave intensity.

materials based on microstructured transmission lines [108], with particular emphasis on highly integrated components. This permits the miniaturization needed to reach the THz frequency range. Indeed, a number of specific applications in engineering have also been further suggested for the transmission-line approach [109–113], but, unfortunately, this does not provide a clear road map to the optical frequency window. It is possible to go further with these developments and try to implement switches within metamaterial elements [114] even if it is challenging to create then in practice, even for microwaves.

Another promising way for the active control over metamaterial properties arises from the use of liquid crystals with wire media [115, 116], exploiting the ease of reconfigurable anisotropy of their arrangement upon application of an external electric field. The resulting reorientation of the liquid-crystal molecules in the vicinity of wires imposes a controllable change in the dielectric environment, varying the effective permittivity of the whole metamaterial quite remarkably.

Although a lot of experimental results quite often explicitly refer to microwaves, they are, however, scalable to higher frequencies as long as the required design methods and material characteristics remain adequate. The natural limitations occurring for circular resonators, closer to the optical part of the spectrum, are mostly due to the difficulties of obtaining measurable magnetic response, resonance frequency saturation and increased dissipation when the size of metallic structures enters the scale of tens of nanometers [46]. A new approach to split-ring type resonators at high frequencies [117] is available and may enable a wide variety of tunable and active metamaterial design in the future.

Generally speaking, the major pathway to tunability of metamaterials includes:

(1) Modification of a basic element of the composite structure, e. g. *a split-ring resonator,* or a cut-wire pair. Using microwaves as a paradigm for possible scaling to the THz and infrared, achieved by introducing a varactor diode as an externally, or nonlinearly, tunable element. This leads to a shift of the split-ring resonator frequency, and for a composite structure, to either magnetic or electric (or both) response by changing the incident power [44, 106, 118, 119]. (2) Selection of a tunable substrate supporting the layers of elements, such as split-ring resonators. Note that specific properties of the substrate achieve the tunable response of the whole structure [120–122]. Similarly, the substrate may change its properties under external illumination. (3) Control of metamaterial properties through engineering the structure geometry which modifies near-field coupling between the elements, the so-called *structural tunability* [123, 124]. As discussed earlier, the possibility of controlling the effective parameters of a metamaterial using nonlinear response of the split-ring resonators has now some provenance [94,95,104], and more recently these ideas been implemented in a novel type of nonlinear tunable structures [107, 125]. A similar approach can be employed for creating *nonlinear electric metamaterials* [126]. It must be acknowledged, however, that such methods become increasingly difficult to implement at higher frequencies. Some other approaches developed very recently employ an analogy with natural materials that demonstrate different properties depending on their specific crystalline structures [124].

Even given these remarks, some of the tuning mechanisms discussed here can be suitable for scaling towards optical wavelengths. Based upon this philosophy, an account will be given of what will be called nonlinear electric and nonlinear magnetic metamaterials using the resonant conditions of a split-ring resonator modified by adding the capacitance of a varactor diode in series with the distributed capacitance, or by introducing an additional gap into which a varactor is placed. The series application of the diode provides a simple mechanism for both tunability and nonlinearity suited to the formation of metamaterials, particularly for magnetic thin-film and microwave nonlinear material developments. The symmetry and simplicity of such systems also lends itself to greater integration, allowing the structure to be translated more readily to the THz and optical frequency domains.

6.1. Nonlinear magnetic metamaterials

Nonlinear magnetic metamaterials operating at microwave frequencies can be fabricated by modifying the properties of split-ring resonators and introducing varactor diodes in each element of the composite structure [44, 106], such that the whole structure becomes dynamically tunable by varying the amplitude of the propagating electromagnetic waves. In this way, it can be demonstrated that the power-dependent transmission of the magnetic metamaterials at higher powers [107, 125], as suggested theoretically [95], and it is possible to realize experimentally the nonlinearity-dependent enhancement or suppression of the transmission in dynamically tunable magnetic metamaterial.

There is a power-induced shift of the magnetic resonance due to the action of varactor diodes that are introduced into split-ring resonators. It can be measured by observing the transmission of a magnetic metamaterial for different values of the input power. The results show that, by selecting an operational frequency near to the resonance, a dynamical change of transmission properties of the metamaterial, by varying the input power, is obtained.

If the parameters of a metamaterial vary and cross the boundary between positive and negative values of the effective magnetic permeability, the structure properties such as transmission will be switched as well, so that the material itself will change from opaque to transparent. The intensity of electromagnetic waves generated by a point source is nonuniform, so that a shift of resonances of individual split-ring resonators is inhomogeneous inside the metamaterial structure. The resonators closer to the source will experience stronger fields and thus only the central part of the metamaterial becomes transparent. The experimental results reveal a narrow aperture of the beam emerging from the metamaterial [125]. In the same metamaterial sample, the opposite effect can be observed, when, at the high-frequency side of the resonance, the transmission is suppressed by the

nonlinearity. While the metamaterial is transparent for low powers, the growth of the wave amplitude makes a part of the metamaterial opaque, thus preventing the radiation from progressing through the sample.

6.2. Nonlinear electric metamaterials

Given that the nonlinear shift of the resonance results for a very strong nonlinear magnetic response for split-ring resonators, a similar approach can be used in the design of *nonlinear electric resonators*, in order to obtain a strong nonlinear electric response [126], but this time two perpendicular sets of boards are deployed [126]. These are introduced to create a relatively isotropic response. Within each resonator, an additional gap is introduced where a varactor diode is placed, introducing an additional series capacitance in order to tune the resonant frequency. The transmission response shows that for the lowest incident power, there is negligible tuning of the response by the incident wave. Hence, the transmission response in this case is essentially linear.

The higher-frequency mode does not shift its frequency with a change of the incident power. This mode consists of two current loops flowing in the same direction, thus their magnetic dipole moments add constructively. As the accumulated charges across the gaps have opposite directions, this results in a vanishing electric dipole moment. As there is no net current through the central conductor, the nonlinear response of the varactor diode does not come into play.

The nonlinear transmission exhibits a significant nonlinear response. In the case of the boards being perpendicular to the direction of propagation, the higher-frequency magnetic stop-band does not exist. This is due to the symmetry of the fields across the gaps and the lack of any magnetic field component normal to the rings. Both resonances are noticeably modified in the isotropic configuration compared to when they are measured separately. This is likely to be due to the strong electrical interaction between the nearest-neighbor boards in the orthogonal directions, due to their gaps being in close proximity. Hence, exploiting nonlinear electric metamaterials offers quite a different option to the magnetic metamaterial case.

6.3. Structural tunability of metamaterials

Finally, a novel approach for efficient control of the transmission characteristics of metamaterials based on structural tunability is discussed. In fact, the concept is rather general, and it is applicable to various metamaterials as long as the effective medium description is valid.

An anisotropic metamaterial is considered based, again, on split-ring resonators, with the expectation of *scaling towards to optical*. For sufficiently dense arrays, the interaction between the elements differs considerably from a dipole approximation, and the specific procedure to calculate the effective permeability was developed earlier [127]; the latter converges correctly to a Clausius–Mossotti approximation in the sparse lattice limit. Consequently, the effect of mutual coupling is enhanced dramatically as compared to conventional materials, and therefore it is particularly suitable to demonstrate the efficiency of lattice tuning.

The most straightforward lattice tuning approach is to vary the lattice constant b. It was shown [127] that the resonance frequency can be impressively shifted in this way, and this prediction has been confirmed by microwave experiments [123]. Accordingly, a slab of metamaterial can be tuned between transmission, absorption and reflection back to transmission. A clear disadvantage of this method is that varying b significantly would imply a corresponding change in the overall dimension of the metamaterial along z, which might be undesirable for certain applications.

A recent paper [124], discusses the basic principles of structural tuning, by changing a periodic lateral displacement of layers in the xy plane, so that the resonators become displaced along x (y, or both) by a fraction of the lattice constant δa per each b distance from a reference layer with respect to the original position. This decreases the overall mutual inductance in the system and leads to a marked gradual increase in resonant frequency, with a maximal effect achieved for a displacement by $0.5a$. Clearly, any further shift is equivalent to smaller shift values until the lattice exactly reproduces itself for the shift equal to a. As a consequence, resonance of the medium can be "moved" across a signal frequency, leading to a drastic change in transmission characteristics. It is clear that for practical applications it is not even necessary to exploit the whole range of lateral shifts – in the above example it is sufficient to operate between $0.1a$ and $0.3a$ where most of the transition occurs.

As experimental proof of concept, a small reconfigurable system is shown in Fig. 16 using GHz frequencies. To minimize undesirable bianisotropic effects, bound to single-split rings, the boards are assembled so that the gaps are oppositely oriented in adjacent layers (see Fig. 16 (left)), resembling the logic of broadside-coupled split-ring resonators [128].

The experimental transmission spectra, shown in Fig. 16 (right), demonstrate excellent tuning of the resonance frequency. Furthermore, comparison of the experimental resonance shift with the theoretical predictions shows [124] that the experimental system demonstrates even higher efficiency. This effect can be explained by accounting for mutual capacitance between the resonators, which is neglected in our theoretical calculations. Indeed, for the broadside-like configuration of rings, mutual capacitance between them is distributed along the whole circumference [128]. Clearly, when the resonators are laterally displaced, the mutual capacitance decreases, so that this effect is added up to the increase of resonance frequency imposed by decreased inductive coupling.

Recently, reconfigurable THz metamaterials have been discussed [129], in which split-rings with cantilever legs have been used to create the building blocks (unit cells) of a metamaterial with a view to generating an important structural response to an applied current or even some change in the ambient temperature. All of this work illustrates how

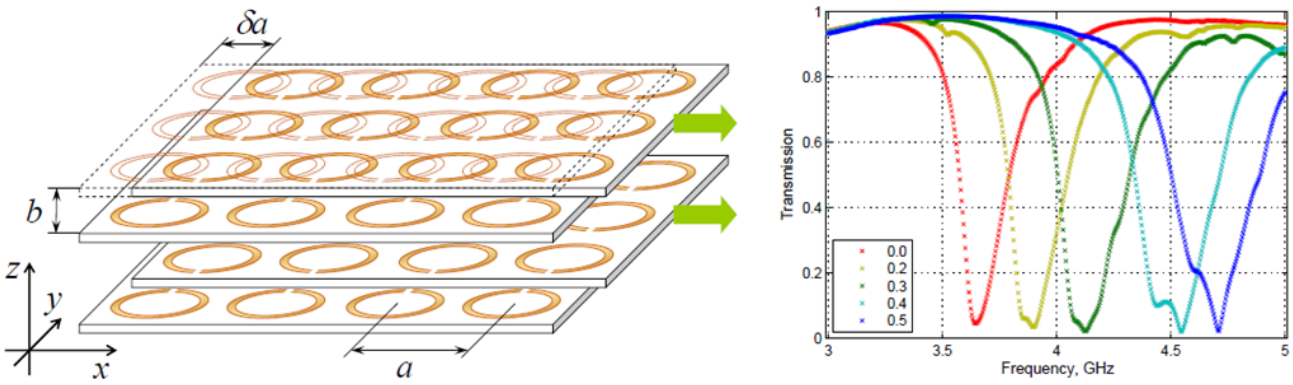

Figure 16 (online color at: www.lpr-journal.org) Left: Schematic of one of the realizations of the lattice tuning concept in metamaterials. Right: Experimental transmission in a waveguide with metamaterial slab at different shifts. Broadside-coupled orientation of layers. Curves with dips from left to right correspond to increasing lattice shift.

much opportunity modern technology is providing for metamaterial manufacturers.

7. Conclusions

In the present review, active and tunable metamaterials are considered. The compensation of losses with gain, and invoking tunable control are aspects of active media that may be connected with either linear or nonlinear media and specific devices. Both linear and nonlinear regimes have their advantages and ranges of applicability.

Loss compensation in metamaterials is a crucial step toward their practical applications. Several promising approaches to loss compensation in metamaterials, and especially negative-phase metamaterial, have been proposed theoretically including optical parametric amplification (OPA) and the addition of gain materials. The properties of many metamaterials critically depend on *surface plasmons*, however, so these are also discussed. Absorption in metals causes damping of *localized* surface plasmons (SPs) and also *propagating* surface plasmon–polaritons (SPPs). This loss can be conquered by optical gain in a dielectric medium adjacent to a metallic surface, or by deploying special nanostructures. The gain discussed here is created by optically pumped dye molecules that, in the vicinity of a silver film, for example, partly emit to the SPP modes. The results of this work pave the way to numerous, acceptable, nanophotonic applications of nanoplasmonics and metamaterials, which otherwise would suffer from strong damping caused by absorption loss in metal constituents, if no action is taken.

A new principle for metamaterials is superheterodyne amplification involving parametric transformation of amplification from a lower to an upper frequency band, provided that some definite linear mechanism of amplification in the lower band can exist. Such a superheterodyne mechanism is very effective for the transformation of gain from slow quasistatic space-charge waves in GaN at THz frequencies to backward electromagnetic waves in the infrared range, propagating in layered metamaterial–semiconductor (GaN) structures.

Negative-phase nanocomposites [130] in the optical range can possess relatively large losses. Therefore, questions concerning the compensation of losses and even amplification of electromagnetic waves in active metamaterials using the different principles of amplification, outlined in the present paper need to be addressed and now become very important for applications in the optical range.

New concepts of active linear metamaterials based on active metaparticles, loaded with active devices are discussed here, implying the possibility of spatial amplification/*convective instability* of electromagnetic waves and therefore the absence of *absolute instability*. This development draws attention to a special class of characteristics for active devices and a recipe for choosing their parameters. This provides for the possibility of spatial amplification, which is achievable, in particular, in the range of negative-phase behavior. Conditions for the absence of absolute instability do not reduce, in any additive manner, in the corresponding conditions for separate active particles, because dispersion characteristics of a medium as a whole have an overriding importance. Instead, a wide class of active materials and a rather general approach for analysis, and/or even "construction" of new forms of them is proposed.

The review also shows the possibility of design of active tunable metamaterials. Tunability can be achieved through tailoring their electromagnetic properties to be dependent on external optical, mechanical, electric or magnetic factors, or control signals. In particular, tunable and nonlinear metamaterials operating at microwave frequencies, can exhibit either nonlinear magnetic, or nonlinear electric, response at microwave frequencies, and they can be created by introducing, for example, a varactor, or backward-wave diode as an externally tunable and nonlinear element within each resonator of the structure. By engineering a resonance of the split-ring resonator, it is possible to modify the averaged response of the composite structure making its parameters dependent on both the external bias and incident power. A novel approach is discussed for an efficient tuning of the transmission characteristics of metamaterials through a continuous adjustment of the lattice structure, i. e. structural

tunability. Finally, even though some of the tuning mechanisms discussed concern applications in the microwave range, it is asserted that they are eminently suitable for scaling upwards to THz, infrared and optical wavelengths.

Acknowledgements. We acknowledge the financial support from the UK Engineering and Physical Sciences Research Council, the Australian Research Council, the Spanish Junta de Andalucía under the project P06-TIC-01368, the NSF PREM grant # DMR 0611430, the NSF CREST grant # HRD 0317722, the NSF NCN grant # EEC-0228390, and the NASA URC grant # NCC3-1035. The authors thank the following for contributions to the research and discussions; J. A. Adegoke, M. Bahoura, V. P. Drachev, M. Gorkunov, A. Kozyrev, M. Mayy, S. Morrison, N. Noginova, V. A. Podolskiy, D. Powell, G. N. Rapoport, K. Reynolds, B. A. Ritzo, I. Shadrivov, C. E. Small, and G. Zhu. A special thank you is extended to R. C. Mitchell-Thomas, who helped create the final document.

Received: 9 June 2010, **Revised:** 29 September 2010, **Accepted:** 1 November 2010

Published online: 6 December 2010

Key words: Metamaterial, active, tunable, gain, nonlinear.

Allan Boardman is Professor of Applied Physics at the University of Salford, Greater Manchester, UK. In addition to possessing a Ph. D., Allan was awarded the degree of Doctor of Science by the University of Durham UK. He is a Fellow of the SPIE and OSA, the UK Institute of Physics and the UK Institute of Mathematics and its Applications. Professor Boardman has made many seminal contributions through his theoretical work on nonlinear wave propagation, including research on surface polaritons, nonlinear guided waves, solitons, magneto-optics, and metamaterials. One of the first to delve into the area of surface plasmons. Although Professor Boardman's work is of fundamental importance to plasmonics, his work combining nonlinear guided waves with magneto-optics has rapidly established him as a leader in the field of nonlinear metamaterials. He delivers many invited conference talks. He has served, for many years, as a Topical Editor for JOSA B on metamaterials, magneto-optics and nonlinear electromagnetic wave theory and is currently Topical Editor for the Journal of Optics on metamaterials and photonic structures.

Volodymyr Grimalsky received the M. Sc. and Ph. D. degrees in physics from Kiev National University, Kiev, Ukraine, in 1982 and 1986, respectively. He worked during 1985–1997 at the Radiophysics Faculty of Kiev National University as the Research Scientist. During 1997–1999, he was Senior Research Scientist at the Space Research Institute, Kiev, Ukraine. During 2000–2006, Dr. Grimalsky was the Titular Researcher at the Electronics Department, INAOE, Mexico. Since 2006, he is the Titular Researcher at CIICAp, Autonomous University of State Morelos (UAEM), Cuernavaca, Mexico. His research interests include electromagnetic and acoustic wave interactions with semiconductors and plasmas, millimeter wave and terahertz devices, electromagnetic monitoring of seismic and volcanic phenomena.

Yuri Kivshar graduated from Kharkov University, Ukraine, with an M. S. in physics, and received his Ph. D. in theoretical and mathematical physics from the Institute for Low Temperature Physics and Engineering, The Ukrainian Academy of Sciences. He has held positions at the Institute for Low Temperature Physics and Engineering in Kharkov, Ukraine (1981–1990), at the Dpto. de Fisica Teorica Universidad Complutense in Madrid, Spain (1990–1991), at the Institute for Theoretical Physics, University of Dusseldorf, Germany (1991–1993) and is currently Professor of the Nonlinear Physics Center, in the Research School of Physics and Engineering, The Australian National University, Canberra, Australia.

Svetlana Koshevaya received her Ph. D. in radiophysics from Kiev Institute of Radioproblems, Kiev University in 1969, and her Dr. Sc. from Kiev University, in 1986. She held various positions at the Kiev Institute of Radioproblems and at the Institute "Orion" and was Principal Lecturer, Associate Professor and Full Professor at the Faculty of Radiophysics of Kiev National University. She was Titular Researcher "C" (1995–1998), in INAOE, Puebla, Mexico. Since 1998, she is Titular Researcher "C" at CIICAp, Autonomous University of State Morelos (UAEM), Cuernavaca, Mexico. Her research interests include remote sensing system, photonics and millimeter-wave integrated technique, nonlinear radiolocation, and solitonics.

Mikhail Lapine is the Coordinating Editor for "Metamaterials" journal and also a researcher at the University of Sevilla, Spain. He has been active in metamaterials research since 2001 and is mostly interested in nonlinear and tunable (reconfigurable) metamaterials as well as metamaterial devices and applications. He acts as a reviewer for several journals and contributes to a number of international conferences, chairing sessions and delivering invited talks.

Natalia Litchinitser received her Ph. D. in Electrical Engineering from the Illinois Institute of Technology, Chicago, in 1997. She has held positions as a Postdoctoral Fellow, Inst. of Optics, University of Rochester, a Senior Member of Technical Staff at Tyco Submarine Systems, a Member of Technical Staff at OFS Labs/Bell Labs, and an Assistant Research Scientist at EECS, University of Michigan. She currently works as an Assistant Professor in the Electrical Engineering Department at the University of Buffalo, the State University of New York. She specializes in nonlinear optics, photonic bandgap structures, photonic crystal fibres, nanostructures and metamaterials

Vadim Malnev is a Professor of Theoretical Physics at Physics Department of Addis Ababa (Ethiopia) University since 2007. He was awarded a degree of a Doctor of Physical Mathematical Sciences at Kiev National University. He has served, for many years, as an Executive Secretary of Ukrainian Journal of Physics. He is a coauthor, jointly with A. Sitenko, of a book "Plasma Physics Theory", Chapman & Hall, London, 1995. He specializes in plasma physics, composite media, and metamaterials.

Mikhail Noginov received his Ph. D. in Physical-Mathematical Sciences from General Physics Institute of the USSR Academy of Sciences (Moscow, Russia) in 1990. His affiliations include:

the General Physics Institute of the USSR Academy of Sciences, Alabama A & M University and Norfolk State University (1997–present). He has published two books, five book chapters and over 100 papers in peer-reviewed journals, and over 100 publications in proceedings of professional societies and conference technical digests. He has served as a chair and a committee member on several conferences of SPIE and OSA. His research interests include metamaterials, nanoplasmonics, random lasers, solid-state laser materials, and nonlinear optics.

Yuriy Rapoport received the M. Sc. and Ph. D. degrees in Theoretical Physics from Kyiv National University, Kyiv, Ukraine, in 1978 and 1986, respectively. He held positions at the Research Institute "Saturn", Kyiv, USSR. Since 1991 he is Senior Research Scientist at Physics Faculty, Kyiv Taras Shevchenko National University, Kyiv, Ukraine. During 1998–2007 he also worked at Institute for Space Research, National Academy of Science of Ukraine, Kiev, Ukraine. He was an Invited Researcher at the University of Electro-communications, Japan, Visiting Professor at The University of Montana, Dillon, Montana, USA, and Visiting Researcher at the University of Salford, UK and in 2010 is Visiting Professor at Aalto University, Finland. His research interests include linear and nonlinear wave processes in layered atmosphere, plasma, ferrite and active metamaterial structures with device applications, modelling wave coupling in the system "lithosphere-atmosphere-ionosphere-magnetosphere (LAIM)" and electromagnetic monitoring of seismoionospheic processes.

Vladimir Shalaev is Professor of Purdue University, in the School of Electrical and Computer Engineering. He earned a doctoral degree in physics and mathematics in 1983 and a master's degree in physics, in 1979, both from the Krasnoyarsk State University in Russia. He has held positions at the University of Heidelberg in Germany, the University of Toronto in Canada, and the New Mexico State University before being appointed Professor at Purdue University. Vlad Shalaev is known worldwide for his ground-breaking work on optical metamaterials and nanophotonics. His group also undertake important work in loss compensation and designs for cloaking devices using transformation optics. He was the recipient of the 2010 Willis E. Lamb Award for Laser Science and Quantum Optics and the 2010 OSA Max Born Award for seminal contributions to both the theoretical framework and experimental realisation of optical metamaterials.

References

[1] A. Scott, Active and Nonlinear Wave Propagation in Electronics (John Wiley & Sons, New York, 1970).
[2] S. Maas, Microwave J. **51**, 34–44 (2008).
[3] J. B. Pendry, Phys. Rev. Lett. **85**, 3966–3969 (2000).
[4] M. Lapine and S. Tretyakov, IET Proc. Microw. Ant, Propagation **1**, 3–11 (2007).
[5] A. D. Boardman, R. C. Mitchell-Thomas, N. J. King, and Y. G. Rapoport, Opt. Commun. **283**, 1585–1597 (2010).
[6] M. Lapine, M. Gorkunov, and K. H. Ringhofer, Phys. Rev. E **67**, 065601 (2003).
[7] Y. S. Kivshar, Nonlinear and Tunable Metamaterials, in: Metamaterials: Fundamentals and Applications II, edited by M. A. Noginov, N. I. Zheludev, A. D. Boardman, and N. Engheta Proc. SPIE **7392**, 739217 (2009).
[8] K. Aydin, Z. F. Li, M. Hudlicka, S. A. Tretyakov, and E. Ozbay, New J. Phys. **9**, 326 (2007).
[9] V. M. Shalaev, W. S. Cai, U. K. Chettiar, H. K. Yuan, A. K. Sarychev, V. P. Drachev, and A. V. Kildishev, Opt. Lett. **30**, 3356–3358 (2005).
[10] K. J. Webb and L. Thylen, Opt. Lett. **33**, 747–749 (2008).
[11] S. Abielmona, S. Gupta, and C. Caloz, IEEE T. Microw. Theory **57**, 2617–2626 (2009).
[12] G. V. Eleftheriades and K. G. Balmain, Negative Refraction Metamaterial: Fundamental Principles and Applications (John Wiley & Sons, Hoboken, 2005).
[13] A. D. Boardman, N. King, and Y. Rapoport, Metamaterials II, Proc. SPIE **6581**, 58108–58108 (2007).
[14] A. D. Boardman and P. Egan, J. Opt. A Pure Appl. Opt. **11**, (2009).
[15] A. D. Boardman, N. King, and Y. G. Rapoport, Circuit Model of Gain in Metamaterials, in: Nonlinearities in Periodic Structures and Metamaterials edited by C. Denz, Y. S. Kivshar, and S. Flach (Springer, Heidelberg, Dordrecht, London, New York, 2009).
[16] M. A. Noginov, V. A. Podolskiy, G. Zhu, M. Mayy, M. Bahoura, J. A. Adegoke, B. A. Ritzo, and K. Reynolds, Opt. Express **16**, 1385–1392 (2008).
[17] A. D. Boardman, Y. G. Rapoport, N. King, and V. N. Malnev, J. Opt. Soc. Am. B **24**, A53–A61 (2007).
[18] A. D. Boardman, N. King, R. C. Mitchell-Thomas, V. N. Malnev, and Y. G. Rapoport, Metamaterials **2**, 145–154 (2008).
[19] A. K. Popov and V. M. Shalaev, Opt. Lett. **31**, 2169–2171 (2006).
[20] A. B. Mikhailovskii, Theory of Plasma Instabilities, Vol. 1: Instabilities of a Homogeneous Plasma (Studies in Soviet Science) (Consultants Bureau, London, 1974).
[21] A. V. Pokhotelov and O. A. Guglielmi, Geoelectromagnetic Waves (Taylor & Francis, New York, 1996).
[22] H. Haken, Synergetics: Introduction and Advanced Topics (Springer, New York, 2004).
[23] J. B. Pendry, A. J. Holden, D. J. Robbins, and W. J. Stewart, IEEE T. Microw. Theory **47**, 2075–2084 (1999).
[24] A. A. Govyadinov, V. A. Podolskiy, and M. A. Noginov, Appl. Phys. Lett. **91**, (2007).
[25] M. A. Noginov, G. Zhu, M. Bahoura, J. Adegoke, C. E. Small, B. A. Ritzo, V. P. Drachev, and V. M. Shalaev, Opt. Lett. **31**, 3022–3024 (2006).
[26] N. Bloembergen, Nonlinear Optics (World Scientific Publishing Company, New York, 1996).
[27] A. K. Popov and V. M. Shalaev, Appl. Phys. B Lasers O. **84**, 131–137 (2006).
[28] Z. G. Dong, H. Liu, M. X. Xu, T. Li, S. M. Wang, S. N. Zhu, and X. Zhang, Opt. Express **18**, 18229–18234 (2010).
[29] X. Z. Wei, H. F. Shi, X. C. Dong, Y. G. Lu, and C. L. Du, Appl. Phys. Lett. **97**, (2010).
[30] N. Stefanou, N. Papanikolaou, and C. Tserkezis, Physica B **405**, 2967–2971 (2010).
[31] V. G. Kravets, F. Schedin, S. Taylor, D. Viita, and A. N. Grigorenko, Opt. Express **18**, 9780–9790 (2010).
[32] M. Dragoman and D. Dragoman, Progr. Quant. Electron. **32**, 1–41 (2008).

[33] B. J. Seo, T. Ueda, T. Itoh, and H. Fetterman, Appl. Phys. Lett. **88**, (2006).
[34] N. Engheta, A. Salandrino, and A. Alu, Phys. Rev. Lett. **95**, (2005).
[35] E. M. Lifshitz and L. P. Pitaevskii, Physical Kinetics (Elsevier, Oxford, 1981).
[36] A. M. Fedorchenko and N. Y. Katsarenko, Absolute and Convective Instability in Plasma and Solid State (Nauka (in Russian), Moscow, 1981).
[37] R. Briggs, Electron-Stream Interactions with Plasmas (MIT Press, Cambridge, Mass, 1964).
[38] C. S. Huang and M. C. Kelley, J. Geophys. Res. Space **101**, 24521–24532 (1996).
[39] Y. G. Rapoport, M. Hayakawa, O. E. Gotynyan, V. N. Ivchenko, A. K. Fedorenko, and Y. A. Selivanov, Phys. Chem. Earth **34**, 508–515 (2009).
[40] N. N. Akhmediev and A. Ankiewicz, Dissipative Solitons (Springer, Berlin, 2005).
[41] N. N. Akhmediev and A. Ankiewicz, Solitons (Chapman & Hall, London, 1997).
[42] A. A. Barybin and V. M. Prigorovsky, Izvestiya VUZ Fizika **24**, 28–41 (1981).
[43] A. A. Barybin, Waves in Thin-Film Semiconductor Structures with Hot Electrons (Nauka (in Russian), Moscow, 1986).
[44] I. V. Shadrivov, S. K. Morrison, and Y. S. Kivshar, Opt. Express **14**, 9344–9349 (2006).
[45] N. M. Litchinitser, I. R. Gabitov, A. I. Maimistov, V. M. Shalaev, and E. Wolf, Negative Refractive Index Metamaterials in Optics, in: Progress in Optics, edited by E. Wolf (Elsevier, Amsterdam, 2008).
[46] V. P. Drachev, U. K. Chettiar, A. V. Kildishev, H. K. Yuan, W. S. Cai, and V. M. Shalaev, Opt. Express **16**, 1186–1195 (2008).
[47] A. Boltasseva and V. M. Shalaev, Metamaterials **2**, 1–17 (2008).
[48] G. Dolling, M. Wegener, C. M. Soukoulis, and S. Linden, Opt. Express **15**, 11536–11541 (2007).
[49] A. K. Popov, S. A. Myslivets, T. F. George, and V. M. Shalaev, Opt. Lett. **32**, 3044–3046 (2007).
[50] G. P. Agrawal, Fiber-Optic Communication Systems (Wiley-Interscience, New York, 2002).
[51] E. Shamonina, V. A. Kalinin, K. H. Ringhofer, and L. Solymar, Electron. Lett. **37**, 1243–1244 (2001).
[52] S. A. Ramakrishna, J. B. Pendry, M. C. K. Wiltshire, and W. J. Stewart, J. Mod. Opt. **50**, 1419–1430 (2003).
[53] S. A. Ramakrishna and J. B. Pendry, Phys. Rev. B **67**, (2003).
[54] S. M. Xiao, V. P. Drachev, A. V. Kildishev, X. J. Ni, U. K. Chettiar, H. K. Yuan, and V. M. Shalaev, Nature **466**, 735–U736 (2010).
[55] T. A. Klar, A. V. Kildishev, V. P. Drachev, and V. M. Shalaev, IEEE J. Sel. Top. Quant. **12**, 1106–1115 (2006).
[56] A. K. Popov and S. A. Myslivets, Appl. Phys. Lett. **93**, (2008).
[57] R. H. Ritchie, Surf. Sci. **34**, 1–19 (1973).
[58] M. Fleischmann, P. J. Hendra, and A. J. McQuilla, Chem. Phys. Lett. **26**, 163–166 (1974).
[59] M. Moskovits, Rev. Mod. Phys. **57**, 783–826 (1985).
[60] H. Raether, Surface Plasmons on Smooth and Rough Surfaces and on Gratings (Springer-Verlag, Berlin, 1988).
[61] A. D. Boardman, Electromagnetic Surface Modes (John Wiley, Chichester, 1982).
[62] N. M. Lawandy, Appl. Phys. Lett. **85**, 5040–5042 (2004).
[63] D. J. Bergman and M. I. Stockman, Phys. Rev. Lett. **90**, 027402 (2003).
[64] M. A. Noginov, G. Zhu, M. Bahoura, J. Adegoke, C. Small, B. A. Ritzo, V. P. Drachev, and V. M. Shalaev, Appl. Phys. B Lasers O. **86**, 455–460 (2007).
[65] V. M. Shalaev, Nonlinear Optics of Random Media: Fractal Composites and Metal Dielectric Films, Springer Tracts in Modern Physics (Springer, Berlin, Heidelberg, 2000).
[66] F. Hide, B. J. Schwartz, M. A. Diaz-Garcia, and A. J. Heeger, Synthetic Met. **91**, 35–40 (1997).
[67] M. P. Nezhad, K. Tetz, and Y. Fainman, Opt. Express **12**, 4072–4079 (2004).
[68] X. Z. Ma and C. M. Soukoulis, Physica B **296**, 107–111 (2001).
[69] J. Seidel, S. Grafstrom, and L. Eng, Phys. Rev. Lett. **94**, 177401 (2005).
[70] W. H. Weber and C. F. Eagen, Opt. Lett. **4**, 236–238 (1979).
[71] K. Ray, H. Szmacinski, J. Enderlein, and J. R. Lakowicz, Appl. Phys. Lett. **90**, (2007).
[72] A. D. Boardman, N. King, and Y. Rapoport, Circuit Model of Gain in Metamaterials, in: Nonlinearities in Periodic Structures and Metamaterials, edited by C. Denz, S. Flach, and Y. S. Kivshar (Springer-Verlag, Berlin, 2009).
[73] F. Auzanneau and R. W. Ziolkowski, IEEE T. Microw. Theory **46**, 1628–1637 (1998).
[74] H. Hartnagel, Semiconductor Plasma Instabilities (Elsevier, New York, 1969).
[75] M. I. Rabinovich and D. I. Trubetskov, Oscillations and Waves: In Linear and Nonlinear Systems (Mathematics and Its Applications) (Springer, London, 1989).
[76] C. Christopoulos, The Transmission-Line Modelling Method (TLM) (IEEE Press, New Jersey, 1995).
[77] B. G. Bosch and R. W. H. Engellmann, Gunn-Effect Electronics (Pitman Publ., London, 1975).
[78] K. K. Ng, Complete Guide to Semiconductor Devices (McGraw-Hill, New York, 1995).
[79] V. F. Oleinik, V. L. Bulgach, V. V. Valyaev, A. V. Zorencko, D. V. Mironov, and V. E. Chaika, Electron Devices of Millimeter and Submillimeter Ranges on the Basis of Nanotechnology (Government University of Information-communication technologies (in Russian), Kiev, 2004).
[80] Y. Ookawa, S. Kishimoto, K. Maezawa, and T. Mizutani, IEICE T. Electron. **E89C**, 999–1004 (2006).
[81] M. P. Shaw, V. V. Mitin, E. Scholl, and H. L. Grubin, The Physics of Instabilities in Solid State Electron Devices (Plenum Press, New York, 1992).
[82] K. Chang, Handbook of Microwave and Optical Components. Vol. 2. Microwave Solid-State Components (John Wiley & Sons, New York, 1990).
[83] S. Y. Liao, Microwave Devices and Circuits (Prentice-Hall Inc, New Jersey, 2002)
[84] R. Bosch and H. W. Thim, IEEE T. Electron. Dev. **ED21**, 16–25 (1974).
[85] G. A. Korn and T. M. Korn, Mathematical Handbook for Scientists and Engineers (McGraw-Hill Book Company, New York, 1968).
[86] Y. V. Gulyaev and Pe. Zilberma, JETP Letters-USSR **11**, 286 (1970).
[87] Y. V. Gulyaev and Pe. Zilberma, Sov. Phys. Solid State, USSR **13**, 798 (1971).
[88] N. Y. Kotsarenko and Y. G. Rapoport, Pisma Zh. Tekh. Fiz. **10**, 843–846 (1984).

[89] S. Koshevaya, J. Escobedo-Alatorre, V. Grimalsky, M. Tecpoyotl-Torres, and M. A. Basurto-Pensado, Int. J. Infrared Millim. Waves **24**, 201–209 (2003).
[90] S. Koshevaya, V. Grimalsky, J. Escobedo-Alatorre, and M. Tecpoyotl-Torres, Microelectron. J. **34**, 231–235 (2003).
[91] J. R. Plumridge, R. J. Steed, and C. C. Phillips, Phys. Rev. B **77**, (2008).
[92] R. W. Boyd, Nonlinear Optics (Academic Press, New York, 1992).
[93] V. V. Grimalsky, S. V. Koshevaya, L. M. Gaggero-S, and F. Diaz-A, J. Infrared Millim. Terahertz Waves **10**, 233–242 (2009).
[94] M. Lapine, M. Gorkunov, and K. H. Ringhofer, Phys. Rev. E **67**, (2003).
[95] A. A. Zharov, I. V. Shadrivov, and Y. S. Kivshar, Phys. Rev. Lett. **91**, 037401 (2003).
[96] M. Lapine and M. Gorkunov, Nonlinear Metamaterials, in: Metamaterials Handbook, edited by F. Capolino (CRC Press, Taylor & Francis Group, Boca Raton, London, New York, 2009).
[97] V. M. Agranovich, Y. R. Shen, R. H. Baughman, and A. A. Zakhidov, Phys. Rev. B **69**, (2004).
[98] M. Lapine and M. Gorkunov, Phys. Rev. E Stat. Nonlin. Soft Matter Phys. **70**, 066601 (2004).
[99] M. V. Gorkunov, I. V. Shadrivov, and Y. S. Kivshar, Appl. Phys. Lett. **88**, (2006).
[100] R. R. A. Syms, L. Solymar, and I. R. Young, Metamaterials **2**, 122–134 (2008).
[101] V. Roppo, M. Centini, D. de Ceglia, M. A. Vicenti, J. W. Haus, N. Akozbek, M. J. Bloemer, and M. Scalora, Metamaterials **2**, 135–144 (2008).
[102] X. Y. Miao, B. Passmore, A. Gin, W. Langston, S. Vangala, W. Goodhue, E. Shaner, and I. Brener, Appl. Phys. Lett. **96**, (2010).
[103] M. J. Dicken, K. Aydin, I. M. Pryce, L. A. Sweatlock, E. M. Boyd, S. Walavalkar, J. Ma, and H. A. Atwater, Opt. Express **17**, 18330–18339 (2009).
[104] M. Gorkunov and M. Lapine, Phys. Rev. B **70**, 235109 (2004).
[105] O. Reynet and O. Acher, Appl. Phys. Lett. **84**, 1198–1200 (2004).
[106] D. A. Powell, I. V. Shadrivov, Y. S. Kivshar, and M. V. Gorkunov, Appl. Phys. Lett. **91**, (2007).
[107] I. V. Shadrivov, A. B. Kozyrev, D. W. van der Weide, and Y. S. Kivshar, Appl. Phys. Lett. **93**, 161903 (2008).
[108] J. Carbonell, V. E. Boria, and D. Lippens, Microw. Opt. Technol. Lett. **50**, 474–479 (2008).
[109] H. Kim, A. B. Kozyrev, A. Karbassi, and D. W. van der Weide, IEEE Microw. Wireless Compon. Lett. **15**, 366–368 (2005).
[110] S. Lim, C. Caloz, and T. Itoh, IEEE T. Microw. Theory **53**, 161–173 (2005).
[111] I. B. Vendik, D. V. Kholodnyak, I. V. Kolmakova, E. V. Serebryakova, and P. V. Kapitanova, Microw. Opt. Technol. Lett. **48**, 2632–2638 (2006).
[112] I. Gil, J. Bonache, J. Garcia-Garcia, and F. Martin, IEEE T. Microw. Theory **54**, 2665–2674 (2006).
[113] E. P. Brennan, A. G. Schuchinsky, and V. F. Fusco, Microw. Opt. Technol. Lett. **48**, 2538–2542 (2006).
[114] Y. E. Erdemli and A. Sondas, J. Electromagnet. Waves **19**, 1907–1918 (2005).
[115] M. V. Gorkunov and M. A. Osipov, J. Appl. Phys. **103**, (2008).
[116] M. G. Silveirinha, P. A. Belov, and C. R. Simovski, Phys. Rev. B **75**, (2007).
[117] V. Delgado, O. Sydoruk, E. Tatartschuk, R. Marqués, M. J. Freire, and L. Jelinek, Metamaterials **3**, 57–62 (2009).
[118] B. N. Wang, J. F. Zhou, T. Koschny, and C. M. Soukoulis, Opt. Express **16**, 16058–16063 (2008).
[119] K. A. Boulais, D. W. Rule, S. Simmons, F. Santiago, V. Gehman, K. Long, and A. Rayms-Keller, Appl. Phys. Lett. **93**, (2008).
[120] S. O'Brien, D. McPeake, S. A. Ramakrishna, and J. B. Pendry, Phys. Rev. B **69**, (2004).
[121] Z. Y. Sheng and V. V. Varadan, J. Appl. Phys. **101**, (2007).
[122] N. H. Shen, M. Kafesaki, T. Koschny, L. Zhang, E. N. Economou, and C. M. Soukoulis, Phys. Rev. B **79**, (2009).
[123] I. V. Shadrivov, D. A. Powell, S. K. Morrison, Y. S. Kivshar, and G. N. Milford, Appl. Phys. Lett. **90**, (2007).
[124] M. Lapine, D. Powell, M. Gorkunov, I. Shadrivov, R. Marques, and Y. Kivshar, Appl. Phys. Lett. **95**, (2009).
[125] I. V. Shadrivov, A. B. Kozyrev, D. van der Weide, and Y. S. Kivshar, Opt. Express **16**, 20266–20271 (2008).
[126] D. A. Powell, I. V. Shadrivov, and Y. S. Kivshar, Appl. Phys. Lett. **95**, (2009).
[127] M. Gorkunov, M. Lapine, E. Shamonina, and K. H. Ringhofer, Eur. Phys. J. B **28**, 263–269 (2002).
[128] R. Marques, F. Mesa, J. Martel, and F. Medina, IEEE T. Antenn. Propag. **51**, 2572–2581 (2003).
[129] H. Tao, A. C. Strikwerda, K. Fan, W. J. Padilla, X. Zhang, and R. D. Averitt, Phys. Rev. Lett. **103**, 147401 (2009).
[130] C. R. Simovski and S. A. Tretyakov, Phys. Rev. B **79**, (2009).